Leibniz-Institute of Freshwater Ecology and Inland Fisheries

Effects of zooplankton carcasses degradation on freshwater bacterial community composition and implications for carbon cycling

Olesya V. Kolmakova https://orcid.org/0000-0003-2694-7545, Michail I. Gladyshev https://orcid.org/0000-0003-2276-3095, Jérémy André Fonvielle https://orcid.org/0000-0002-8077-2419, Lars Ganzert, Thomas Hornick https://orcid.org/0000-0003-0280-9260, Hans-Peter Grossart https://orcid.org/0000-0002-9141-0325

DOI
10.1111/1462-2920.14418

Original publication date
24 September 2018

Document version
Accepted version

Published in
Environmental Microbiology

Citation (Vancouver)
Kolmakova OV, Gladyshev MI, Fonvielle JA, Ganzert L, Hornick T, Grossart H-P. Effects of zooplankton carcasses degradation on freshwater bacterial community composition and implications for carbon cycling. Environmental Microbiology. 2019;21(1):34-49.

Effects of zooplankton carcasses degradation on freshwater bacterial community composition and implications for carbon cycling

Olesya V. Kolmakova[1,2,3*], Michail I. Gladyshev[1,2], Jérémy André Fonvielle[3], Lars Ganzert[3,4,5], Thomas Hornick[3] and Hans-Peter Grossart[3,6]

[1] Institute of Biophysics of Siberian Branch of Russian Academy of Sciences, Akademgorodok, 660036 Krasnoyarsk, Russia

[2] Siberian Federal University, Svobodny av. 79, 660041 Krasnoyarsk, Russia

[3] Leibniz-Institute of Freshwater Ecology and Inland Fisheries (IGB), Department of Experimental Limnology, Alte Fischerhütte 2, 16775 Stechlin, Germany.

[4] GFZ German Research Centre for Geosciences, Helmholtz Centre Potsdam, Section 5.3 Geomicrobiology, 14473, Potsdam, Germany.

[5] University of Göttingen, Experimental Phycology and Culture Collection of Algae (SAG), Nikolausberger Weg 18, 37073 Göttingen, Germany.

[6] University of Potsdam, Institute of Biochemistry and Biology, Am Neuen Palais 10, 14469 Potsdam, Germany.

*Corresponding author: kolmoles@ibp.krasn.ru, ORCID 0000-0003-2694-7545

Running title: Effect of dead zooplankton on bacteria and C-cycle

Originality-Significance Statement

In a recent comprehensive review on the role of zooplankton in the aquatic carbon cycle, Steinberg and Landry (2017) state that the carbon input via carcasses, in spite of their abundance, remains largely unknown. Our study is the first to cast light upon this important yet overlooked organic matter source for microorganisms in aquatic systems. Our study reveals that decomposing zooplankton carcasses could be a major driver of bacterial community composition in many aquatic ecosystems, e.g. in lakes with an inverted biomass pyramid and in common events of mass zooplankton mortality. Using stable isotope labeling we show that zooplankton carcasses are well degraded by heterotrophic prokaryotes indicating their labile nature, but do not significantly stimulate the degradation of more refractory organic matter such as humic matter. Thus, carcasses are important hotspots of microbial activity influencing the organic matter sinking flux and overall microbial diversity in aquatic ecosystems.

Summary

Non-predatory mortality of zooplankton provides an abundant, yet, little studied source of high quality labile organic matter (LOM) in aquatic ecosystems. Using laboratory microcosms, we followed the decomposition of organic carbon of fresh ^{13}C-labelled *Daphnia* carcasses by natural bacterioplankton. The experimental setup comprised blank microcosms i.e. artificial lake water without any organic matter additions (**B**), and microcosms either amended with natural humic matter (**H**), fresh *Daphnia* carcasses (**D**) or both, i.e. humic matter and *Daphnia* carcasses (**HD**). Most of the carcass carbon was consumed and respired by the bacterial community within 15 days of incubation. A shift in the bacterial community composition shaped by labile carcass carbon and by humic matter was observed. Nevertheless, we did not observe a quantitative change in humic matter degradation by heterotrophic bacteria in the presence of LOM derived from carcasses. However, carcasses were the main factor driving the bacterial community composition suggesting that the presence of large quantities of dead zooplankton might affect the carbon cycling in aquatic ecosystems. Our results imply that organic matter derived from zooplankton carcasses is efficiently remineralized by a highly specific bacterial community, but doesn't interfere with the bacterial turnover of more refractory humic matter.

Introduction

The global carbon cycle is one of the most important biogeochemical processes regulating the climate on our planet (Ward *et al.*, 2013). In particular, carbon fluxes between aquatic and terrestrial ecosystems constitute a key component of global biogeochemical cycles (Pace *et al.*, 2004; Battin *et al.*, 2009; Ward *et al.*, 2013). Nowadays, it is well known that a significant part of terrigenous organic matter drains from soils into aquatic ecosystems, especially in the boreal zone (Vachon *et al.*, 2017). Freshwaters are considered hotspots of organic matter degradation, sustaining a shorter half-life of organic carbon compared to terrestrial and marine ecosystems (Catalán *et al.*, 2015). In freshwaters, organic matter comprises a heterogeneous mixture of different carbon sources with varying degradability. Depending on their degradability by aquatic microbes, the drained terrigenous organic matter is buried to a variable extent in sediments of aquatic ecosystems (Tranvik *et al.*, 2009). However, most of the terrigenous (allochthonous) organic carbon is transported into aquatic ecosystems in the form of refractory organic matter (ROM) resulting in a generally higher retention time due to its slow decomposition by aquatic microorganisms (Bianchi, 2011). A major part of this ROM in freshwater ecosystems is represented by humic matter (Rocker *et al.*, 2012a).

Bacterial species differ in their response to various sources of carbon resulting in profound implications for aquatic carbon cycling. It has been demonstrated that the availability of organic matter promotes growth of both generalist species, which are able to degrade a wide range of substrates, as well as highly specialized populations degrading specific substrate fractions (Hutalle-Schmelzer *et al.*, 2010). Dead zooplankton, which used to be generally neglected in aquatic ecology due to methodological limitations (Tang *et al.*, 2009, 2014), is an overlooked and highly abundant source of labile carbon in most freshwater ecosystems. Zooplankton carcasses represent a high quality organic substrate for

heterotrophic bacteria due to their relatively low C:N:P ratio as compared to phytoplankton and detritus (Tang *et al.*, 2014). Consequently, zooplankton carcasses are "hot spots" of activity of pelagic microorganisms consuming labile organic matter (LOM) as well as ROM (Tang *et al.*, 2006; Grossart *et al.*, 2007; Elliott *et al.*, 2010; Kirillin *et al.*, 2012). However, zooplankton carcasses provide not only a carbon source for microorganisms, but also surfaces for attachment. Microorganisms attached to particles are situated in close spatial proximity and can benefit from extracellular degradation enzymes released in the environment (Catalán *et al.*, 2015). Thus, attached microorganisms have a higher capacity to degrade polymeric organic matter than their free living counterparts (Grossart, 2010). Consequently, zooplankton carcasses are selecting for specific, but yet uncharacterized microbial communities (Tang *et al.*, 2010). The complex LOM of zooplankton carcasses constitutes a valuable source of nutrients and energy for microorganisms, thus implying effects on aquatic carbon cycling, in particular of the more refractory carbon pools. For instance, carcass LOM may induce a "priming effect" and facilitate the degradation of ROM (Bianchi, 2011).

Thus, our primary objective was to investigate consequences on bacterial community composition and carbon cycling in aquatic ecosystems after input of zooplankton carcasses. Since the quality of available organic matter can be a selective force for bacterioplankton community composition (Gómez-Consarnau *et al.*, 2012), we tested the hypothesis that nutrient-rich LOM provided by *Daphnia* carcasses selects for generalist bacteria in contrast to C-rich ROM selecting to a larger extent for specialists. In a microcosms experiment, we observed the degradation of ^{13}C-labeled carcasses by heterotrophic bacteria from a dystrophic humic bog lake in the presence of indigenous humic matter (treatment **HD**) to track the fate of carcass carbon (Fig. S1). In parallel, we followed three control treatments with either *Daphnia* carcasses (**D**) or humic matter (**H**) as a sole carbon source, and a blank treatment (**B**) containing solely a natural bacterial community. We used optical properties (specific UV absorbance at 254 nm – $SUVA_{254}$, humification index, etc.) and size exclusion

99 chromatography to analyze the influence of carcasses on the dissolved organic matter (DOM)
100 pool and combined it with 16S rRNA gene Illumina amplicon sequencing to characterize the
101 bacterial community composition in detail.

102 **Results**

103 **Microbial dynamics and community composition**

104 *Daphnia* carcasses showed a rapid decomposition during the first week of incubation,
105 with visible changes in the state of carcasses over time (Fig. S2a-d). At the end of the
106 experiment, the carcasses were still visible as disintegrated parts of the carapace. Dense
107 bacterial colonization of the carcasses was observed (Fig. S2e), while protist grazers or
108 autotrophic organisms were not detected indicating that protozoan grazers and large
109 phytoplankton have been successfully removed by the pre-filtration step. No differences in
110 bacterial counts were observed in the **B** microcosms between the start and the end of the
111 experiment (Table 1). However, a clear increase in bacterial cells counts was observed in **H**,
112 **D** and **HD** microcosms (43%, 654% and 617%, respectively; Table 1). This indicated a higher
113 bacterial growth in the presence of *Daphnia* carcasses and a slower growth on humic matter
114 alone. At the same time, bacterial cell counts did not significantly differ between **HD** and **D**
115 microcosms (paired t-test, $p > 0.05$, Table 1).

116 After sequencing and performing a quality check for all samples, 595036 reads of 16S
117 rRNA gene fragments were obtained that clustered into 1161 bacterial operational taxonomic
118 units (OTUs). The identified OTUs belonged to 26 known phyla (Fig. 1). In the initial
119 bacterial inoculum from Lake Grosse Fuchskuhle, *Proteobacteria* was the dominant phylum
120 (48% of all sequences), with a high proportion of the class *Betaproteobacteria* (30% of all
121 sequences). By the end of the experiment, the relative abundance of *Proteobacteria* increased

122 in all treatments, especially in carcasses amended microcosms (**HD** and **D**; Fig. 1), with a
123 dominance of the class *Gammaproteobacteria* (62 % and 50 % in **HD** and **D** respectively).

124 At the end of the experiment, the microcosms **HD** and **D** had a lower OTU richness
125 and evenness compared to microcosms without added carcasses (**H** and **B**; Table 2).
126 Microcosms **H** had lower species richness than **B** microcosms, but showed a higher evenness
127 (Table 2).

128 In an unconstrained ordination (Fig. 2), all treatments were distinguishable from one
129 another and from the initial inoculum (ANOSIM, R = 0.835, p = 0.001). The OTUs
130 accounting for most of the difference between the treatments were identified using a SIMPER
131 test (Table 3). The relative abundance of the most influential OTU (OTU1, *Pseudomonas* sp.)
132 was significantly different between the start and the end of the incubation for all treatments
133 (ANOVA $F_{4,15}$ = 102.89, $p < 0.001$). The distribution of different OTUs in all treatments is
134 discussed in more details in the Supplementary Information.

135 **DOM composition and fate of carcass carbon**

136 We aimed to test for the "priming effect" by comparing the predicted total organic
137 carbon degradation rate (ΔTOC) in **HD** microcosms, calculated from ΔTOC in the control
138 microcosms **D**, **H**, and **B**, to the measured ΔTOC in **HD** microcosms (see Supplementary
139 Methods for more details). The predicted ΔTOC was -1.015 ± 0.115 mg L^{-1} and did not differ
140 significantly (paired t-test, $p > 0.05$) from the ΔTOC measured in **HD** microcosms (-1.094 ±
141 0.057 mg L^{-1}).

142 During carcass decomposition (in **HD** and **D** microcosms only), the particulate organic
143 carbon (POC) decreased approximately four-fold compared to the initial values (Table 1).
144 Nevertheless, no significant differences in concentrations of dissolved organic carbon (DOC),
145 high- and low-molecular weight substances (HMWS and LMWS, respectively) or humic
146 substances were found throughout the experiment in any treatment (paired t-tests, $p > 0.05$ in

147 all tests, Table 1). However, in ROM supplemented microcosms (**HD** and **H)** we observed
148 trends of decreasing concentrations in polysaccharides, amphiphilic molecules, and building
149 blocks of humic substances (Table 1).

150 The $SUVA_{254}$, spectral slopes and optical indices values were not different between
151 the humic-amended microcosms **H** and **HD** (Table 1), and they did not differ between **D** and
152 **B** microcosms (Table 1). An exception was the freshness index, being an indicator for
153 recently produced DOM (Hansen *et al.*, 2016), which was lower in **D** compared to **B**
154 microcosms. Expectedly, the ratio of peakA to peakT, which is known as an indicator of the
155 ratio of humic-like (recalcitrant) to freshly produced (labile) organic matter (Hansen *et al.*,
156 2016), was higher in **H** microcosms compared to **HD** (Wilcoxon test, p-value = 0.03).

157 The carcasses had an average $^{13}C/^{12}C$ ratio of 0.168 ± 0.004 ($\delta^{13}C$ = 13945.3 ±
158 303.9‰). According to this specific signature, the amount of processed carbon originating
159 from the carcasses was computed in all carcass-containing microcosms (i.e. **HD** and **D**). In
160 **HD** microcosms, 72.8% of POC and 2.2% of DOC originated from *Daphnia* carcasses,
161 against 82.1% of POC and 21.1% of DOC for the **D** microcosms (Fig. 3).

162 The bacterial respiration, measured as the increase in CO_2 and normalized to the
163 background respiration (i.e. respiration from the blank microcosms **B**) was higher in **D**
164 microcosms compared to **H** but lower compared to **HD** microcosms (Fig. S3). The respiration
165 per amount of initially added carbon and normalized to the background respiration was higher
166 in **HD** microcosms compared to **H** but lower compared to **D** microcosms, and was used to
167 confirm the labile character of the organic matter originating from the zooplankton carcasses.
168 All differences in CO_2 concentrations between the microcosms were significant (1-way
169 ANOVA $F = 241.6$, $p < 0.001$; Tukey post hoc test $p < 0.01$ for all pairs).

170 To test for the priming effect, the predicted $^{13}C/^{12}C$ ratio in the respired CO_2 of **HD**
171 microcosms was calculated from the values in the control microcosms **D**, **H**, and **B**, and
172 compared to the measured $^{13}CO_2/^{12}CO_2$ ratio in **HD** microcosms (see Supplementary Methods

173 for more details). The predicted $^{13}CO_2/^{12}CO_2$ ratio for **HD** (0.078 ± 0.003) did not differ
174 significantly (paired t-test, $p > 0.05$) from the measured value (0.073 ± 0.003). In **HD**
175 microcosms, 87.8 ± 6.3 % of respired CO_2 originated from zooplankton carcasses when
176 normalized to the background respiration of microcosms **B.**

177 **Interactions between microbial community and DOC quality**

178 The interactions between bacterial community composition and DOC quality in
179 microcosms **HD**, **H**, and **D** revealed specific patterns in bacterial substrate preferences (Fig.
180 4). The connections between bacterial genera and DOC qualities significantly differed
181 between microcosms **H** and **D** (Fig. 4a). Thus, bacteria positively interacting with DOC
182 concentration as well as humification and fluorescence indices are the ones thriving in the
183 presence of humic matter (Fig. 4a). On the contrary, bacteria negatively associated with these
184 parameters are favored by carcasses (Fig. 4a). Similarly, genera positively correlated with
185 DOC concentration, fluorescence index and A/T peak ratio (Fig. 4b, comparing microcosms
186 **HD** and **D**) seem to be favored by humic matter when *Daphnia* carcasses are available.
187 However, those genera negatively correlated with these parameters are suppressed by humic
188 matter in the presence of carcasses.

189 **Discussion**

190 The main objective of this study was to track the degradation of zooplankton
191 carcasses, as a so far largely neglected but common and labile carbon source (Tang *et al.*,
192 2014). Our study reveals selection of defined bacterial communities in the presence of
193 carcasses strongly related to the specific DOM quality released from carcasses. However,
194 carcass-induced availability of LOM and related shifts in bacterial community composition
195 did not result in significant changes in the turnover of the added ROM pool. Consequently,
196 our data do not support a "priming effect" (Bianchi *et al.*, 2011) of refractory humic matter

197 removal in the presence of relatively labile carbon from *Daphnia* carcasses. Nevertheless, the
198 bacterial community composition was greatly affected by the presence of carcass carbon.
199 Thus, our study adds new quantitative and qualitative data on bacterial carbon utilization
200 related to changes in the community composition induced by changes in substrate quality, i.e.
201 addition of zooplankton carcasses, and adds new insights in microbial-organic matter
202 interactions.

203 **Bacterial community composition depending on carbon source**

204 As outlined above, we did not measure any quantitative changes in organic matter
205 degradation between **HD** microcosms and the predicted values calculated based on the
206 parameters of single-carbon source microcosms **H** and **D**. Consequently, the presence of
207 LOM from *Daphnia* carcasses did not change the degradation of humic matter but rather
208 influenced the bacterial community.

209 According to our data on beta-diversity of bacterial assemblages (Fig. 2), the type of
210 treatment strongly affected the bacterial community composition in each microcosm. In
211 microcosms with no extra organic matter addition (**B**), the bacterial community remained
212 similar to the initial inoculum indicating that experimental changes in environmental
213 conditions did not modify the bacterial community composition drastically (Fig. 2). Overall,
214 the addition of carcass LOM was the main driver of the bacterial community composition in
215 the **D** and **HD** microcosms (Fig. 2). Bacterial taxa introduced into the microcosms with the
216 carcasses may also have an effect on bacterial community composition and richness.
217 However, according to literature data, zooplankton carcasses are not primarily decomposed by
218 their native-associated bacterial communities, but rather by ambient bacteria (Bickel and
219 Tang, 2010). This notion is also reflected by the fact that bacteria richness is the lowest in the
220 **HD** and **D** treatments. Thus, in natural waters with a high amount of dead zooplankton,
221 carcasses can be a primary factor driving bacterioplankton community composition with

222 potential effects for carbon cycling. In many lakes with an "inverted" biomass pyramid,
223 zooplankton biomass is higher than phytoplankton biomass (Heathcote *et al.*, 2016). We
224 suppose that the same pattern for dead biomass would indicate that zooplankton and not algal
225 LOM, which is usually in the researcher's focus (Hoikkala *et al.*, 2016; Landa *et al.*, 2016),
226 could be the major driver for bacterioplankton community composition in such ecosystems. In
227 lakes with a "normal" biomass pyramid, zooplankton may still play an important role for
228 determining bacterial community composition in the occasional events of mass zooplankton
229 mortality (Tang *et al.*, 2014). It would be interesting to test this presupposition in further
230 studies. The co-presence of ROM also contributed to specific bacterial communities by
231 selecting for a number of specific OTUs. The observed, significant difference in bacterial
232 community composition between all treatments points to a pronounced effect of substrate
233 quality on bacterial community composition and might result in functional differences.

234 The prevalence of *Betaproteobacteria* in the initial inoculum and in microcosms **B** and
235 **H** (Fig. 1) was in accordance with previous studies on Lake Grosse Fuchskuhle (Grossart *et*
236 *al.*, 2008; Hutalle-Schmelzer *et al.*, 2010). Indeed, *Betaproteobacteria* are among the most
237 numerous bacteria in the upper layers of freshwater lakes, in particular of peat bog lakes
238 (Newton *et al.*, 2011). Moreover, the dominance of *Gammaproteobacteria* in carcass-
239 amended microcosms (Fig. 1) was also expected according to previous studies (Tang *et al.*,
240 2009; Shoemaker and Moisander, 2015). *Gammaproteobacteria* include many species with a
241 copiotrophic lifestyle that can grow faster than the average lake bacterioplankton, especially
242 under nutrient-rich conditions as can be found on carcasses (Newton *et al.*, 2011).
243 Interestingly, a more distinct community pattern emerged in the different microcosms when
244 taking the level of individual OTUs into account. This indicates a close relationship between
245 organic carbon quality and bacterial community structure (Attermeyer *et al.*, 2014, 2015).

246 **Links between organic matter quality and microbial community composition**

247 A number of uncultivated bacterial taxa belonging to the order *Sphingobacteriales*
248 were positively selected solely in the presence of carcasses only (Fig. 4a). Many members of
249 *Sphingobacteriales* express chitinolytic activity (Kämpfer, 2015), but no information is
250 available in particular about the ecological role of the uncultivated representatives found in
251 the present study. High abundances of the NS11-12 marine group were previously associated
252 with an increase in chlorophyll *a* concentration (Meziti *et al.*, 2015) and number of particles,
253 while it is negatively correlated with nitrate concentration (Henson *et al.*, 2016). Moreover,
254 the uncultured bacterial group OPS 17 was previously found not to respond to terrestrial
255 DOM additions (Lindh *et al.*, 2015).

256 Another group of bacteria favored by zooplankton carcass LOM were ubiquitous
257 chemoorganotrophs belonging to genera *Brevundimonas* and *Aeromonas* (Segers *et al.*, 1994).

258 Among the bacteria favored by humic matter (Fig. 4b), genera involved in nitrogen
259 fixation (*Bradyrhizobium*, *Rhizobacter*, unclassified *Rhizobiales*) (Kuykendall, 2005; Goto,
260 2015), organic pollutants degraders *Rhodococcus* (Bell *et al.*, 1998), unclassified
261 *Sphingomonadales* and methylotrophs (uncultured strain PRD01a011B from
262 *Methylophilaceae* (Doronina *et al.*, 2014)) were detected. To a large extent the same bacterial
263 genera were favored by humic matter regardless whether zooplankton carcasses were present.
264 In contrast, bacteria suppressed by humic matter in the presence of carcasses were almost
265 exclusively chemoorganotrophic generalists (Johansen *et al.*, 2005; O'Sullivan *et al.*, 2005;
266 Song *et al.*, 2008; McBride, 2014; Evtushenko, 2015).

267 Besides selecting for certain bacterial populations, zooplankton carcasses strongly
268 decreased the species richness and evenness of the bacterial community (Table 2). Therefore
269 it appears that the availability of a high quality and abundant LOM source can reduce the
270 biodiversity by favoring a small number of copiotrophs dominating the community: in the

271 present study about half of all sequences in the **HD** and **D** microcosms belonged to a single
272 OTU (OTU 1, *Pseudomonas sp.*). In a similar study of Blanchet et al. (2017), the bacterial
273 diversity was not affected by amino acid additions, possibly because free amino acids are
274 simple compounds which can be consumed simultaneously by many members of the
275 community (Trusova et al., 2012). Thus, this pattern can be best explained by the fact that
276 zooplankton carcasses provide microbial habitats and complex, yet labile carbon sources
277 shifting the overall bacterial community towards a less diverse, more uneven, and more
278 copiotrophic community.

279 **Microbial carcass decomposition in relation to carbon quality**

280 An abrupt increase of LOM availability following mass zooplankton mortality
281 commonly observed in natural waters (reviewed by Tang et al. 2014), leads to a substantial
282 input of both DOC and POC. In agreement with a previous study (Tang *et al.*, 2006) *Daphnia*
283 carcasses lost their mostly labile internal tissues rapidly, whereas the chitin-based carapace
284 was more resistant to dissolution and microbial decomposition (Fig S2).

285 However, in our study the leached fraction was rapidly consumed by numerous
286 ambient bacteria (Table 1), and did not increase the DOC concentration significantly in the
287 microcosms with zooplankton carcasses (**D** and **HD**). This statement is supported by our
288 observation that adding 1.334 ± 0.038 mg C L^{-1} with *Daphnia* carcasses resulted in only 0.055
289 ± 0.011 and 0.065 ± 0.010 mg C L^{-1} of carcasses-derived DOC in **D** and **HD** microcosms,
290 respectively (Fig. 3).

291 On the other hand, the chitin-based structure of the carapace was only partially
292 degraded and also used a surface for attachment. At the end of the experiment, 0.270 ± 0.014
293 and 0.258 ± 0.007 mg C L^{-1} originating from *Daphnia* carcasses (19-20% of the initial
294 quantity) remained in the POC fraction of the **D** and **HD** microcosms, respectively (Fig. 3),
295 mainly represented by the remaining carapace and the bacterial biomass (Fig. S2). This is

296 further confirmed by the finding that bacterial taxa degrading chitin were greatly favored in
297 the presence of carcasses at the end of the incubation (Fig. 4). The difference between non-
298 carcass-derived POC in microcosms **D** and **HD** (0.059 ± 0.003 and 0.096 ± 0.003 mg L^{-1},
299 respectively; Fig. 3) presumably occur due to humic matter aggregation converting DOC into
300 POC. This assumption is supported by a two-fold POC increase in the **H** microcosms
301 compared to the initial value (Table 1).

302 In our experiment we used 40 *Daphnia* carcasses per liter, a high but still natural value
303 (Dubovskaya *et al.*, 2003). Most of the organic carbon originating from carcasses was
304 respired by the bacterial community within the two weeks of incubation. Therefore, in natural
305 systems, the considerable amount of LOM released by zooplankton carcasses (Tang *et al.*,
306 2014), can directly affect the functioning of the ecosystem by accelerating microbial carbon
307 turnover and respiratory carbon losses to the atmosphere at short time scales. The more
308 recalcitrant part of the carapace may persist for a longer time, and eventually escapes the
309 water column to be further processed in the sediments (Tang *et al.*, 2014), being also
310 important for carbon sequestration. Consequently, the balance between microbial degradation
311 of zooplankton carcasses and organic matter storage in sediments has a great influence on the
312 aquatic carbon cycle.

313 **Priming, a concept under debate in aquatic sciences**

314 Humic matter was chosen as a recalcitrant carbon source for its ubiquity in aquatic
315 ecosystems and as an important part of the carbon pool in the global carbon cycle. Humic
316 matter can represent up to 80% of the total DOM in freshwaters (Rocker *et al.*, 2012a).
317 Although humic matter is considered as recalcitrant, it can at least partially be decomposed by
318 bacteria (Hutalle-Schmelzer *et al.,* 2010; Rocker *et al.*, 2012a; Kisand *et al.*, 2013).
319 Furthermore, the degradation of humic acids by marine and estuarine bacterial communities
320 seems to be favored by specific environmental conditions, e.g. along a salinity gradient

321 (Rocker *et al.*, 2012a; Rocker *et al.*, 2012b; Kisand *et al.*, 2013). Consequently, recalcitrance
322 and lability of organic matter are not *per se* intrinsic chemical characteristics (Schmidt *et al.*,
323 2011), and may only account for specific environmental settings (Bianchi *et al.*, 2015).

324 In our experiment, we incubated *Daphnia* carcasses and humic matter in different
325 combinations to test for a priming effect of bacterial degradation of ROM induced by the
326 addition of carcass LOM. The addition of a mixture of natural humic matter and *Daphnia*
327 carcasses resulted in the degradation of organic matter and an isotopic ratio of the respired
328 CO_2 similar to what we predicted based on our linear addition model with humic matter or
329 carcasses as the sole carbon source. Moreover, based on DOM characterization (Table 1), the
330 natural humic matter from Lake Grosse Fuchskuhle was only little degraded by bacteria,
331 irrespective of LOM addition via *Daphnia* carcasses. Consequently, and in agreement with
332 previous studies (Bengtsson *et al.*, 2014; Catalán *et al.*, 2015; Dorado-García *et al.*, 2015), we
333 could not detect any quantitative changes in bacterial ROM degradation when using carcass
334 LOM as a potential primer (Table 1).

335 Recently, a number of studies have investigated the prevalence of a priming effect in
336 aquatic ecosystems (e.g., van Nugteren *et al.*, 2009; Guenet *et al.*, 2013; Kuehn *et al.*, 2014;
337 Steen *et al.*, 2015). Various types of ecosystems (marine, lentic, lotic) and habitats (pelagic,
338 hyporheic, sediments) have been tested, as well as different sources of LOM (carbohydrates,
339 algae leachate, gastropod mucus, etc.) and ROM (terrestrial plant tissues, lignocellulose,
340 humic matter, etc.) have been used. Although some authors have found support for ROM
341 priming by more labile organic matter, mainly of algal origin (van Nugteren *et al.*, 2009;
342 Guenet *et al.*, 2013; Hotchkiss *et al.*, 2014; Bianchi *et al.*, 2015; Gontikaki *et al.*, 2015),
343 others did not reveal any evidence for a positive priming effect (Bengtsson *et al.*, 2014;
344 Catalán *et al.*, 2015; Dorado-García *et al.*, 2015; Blanchet *et al.*, 2017), or even found a
345 negative priming effect (Gontikaki *et al.*, 2013) with ROM being decomposed slower in the
346 presence of a labile carbon source. Thus, it appears that the absence or presence of the

347 priming effect may strongly depend on specific environmental or experimental conditions,
348 which may also explain the absence of humic matter degradation in our HD treatments using
349 *Daphnia* carcasses LOM as the primer.

350 **Limitations and applications of the study**

351 The degradation of ROM (such as humic matter) is a combination of two main
352 processes: microbial and photochemical decomposition (Amado *et al.*, 2015). The most
353 efficient humic matter microbial degraders in aquatic systems are fungi (Grinhut *et al.*, 2007).
354 Generally, fungi have a higher capacity then bacteria to synthesize the extracellular oxidative
355 enzymes involved in ROM degradation and thus more readily and successfully initiate humic
356 matter degradation (Rojas-Jimenez *et al.*, 2017). In contrast, bacteria join the process later as
357 degraders of humic matter metabolites (Grossart and Rojas-Jimenez, 2016; Rojas-Jimenez *et*
358 *al.*, 2017). Due to our pre-filtration step to avoid the presence of protozoan grazers and large
359 phytoplankton as has been frequently done in similar incubation experiments (Fonte *et al.*,
360 2013; Guenet *et al.*, 2013; Attermeyer *et al.*, 2014, 2015; Blanchet *et al.*, 2015), fungi, which
361 could potentially constitute an important component of the aquatic priming effect, were
362 removed.

363 Photochemical degradation can break down/oxidise recalcitrant DOM compounds,
364 such as fulvic and humic substances, into more labile molecules (Spencer *et al.*, 2009;
365 Stubbins *et al.*, 2010). It is likely that in natural systems photochemical and microbial
366 degradation work synergistically and thus contribute to the priming effect. On the other hand,
367 UV radiation can also affect biodegradability of LOM in the presence of humic matter
368 (Tranvik and Kokalj, 1998). Our study was conducted in the dark as in other priming effect
369 studies (e.g. Bianchi *et al.*, 2015; Catalán *et al.*, 2015) to avoid photosynthesis which could
370 have obstructed the detection of differences in carbon oxidation between treatments and
371 controls. Thus, it is clear that photodegradation of humic substances was not taken into

account in the present study and might have reduced our possibilities to measure a positive priming effect. However, our study is directly applicable to the situation when the zooplankton carcasses are sinking into the pelagic zone at depths with very low light penetration.

The incubation temperature in our experiment was relatively high (20°C) and not typical for deep waters. Nevertheless, if temperature might have a strong influence on bacterial community composition and its activity (Adams *et al.*, 2010), a lower temperature only slows down the degradation process but not the biodegradability of carcasses. Therefore, in natural systems, the potential of zooplankton carcasses to release a consequential amount of carbon in the atmosphere and to select for specific bacterial community might happen over longer time scales than the ones observed in our experiment.

Another factor that can affect DOM degradation is the oxygen concentration, which usually decreases sharply with depth in the pelagic zone of humic lakes. In our experimental microcosms we maintained 100% oxygen saturation due to mixing with headspace air. However, Tang *et al.* (2006) observed only a small difference between microbial communities decomposing carcasses in anaerobic vs. aerobic conditions, presumably because zooplankton carcasses represent anoxic microenvironments even when oxygen is abundant in the surrounding waters (Glud *et al.*, 2015).

Although the experimental set-up might have its limitations, our findings are relevant to natural environments such as the metalimnion of humic lakes and other deep water layers where the maximum percentage of dead zooplankton is found (Dubovskaya *et al.*, 2018).

Conclusions

We observed a pronounced change in bacterial community composition in microcosms induced by the addition of *Daphnia* carcasses and humic matter. While the quality of both

396 added carbon sources played a role, zooplankton carcasses were the major driver of bacterial
397 community assembly. Even though no priming effect was detected, it is critical to continue
398 studies on ROM degradation in the presence of zooplankton carcasses to better understand
399 microbial dynamics and thus potential changes in organic matter fluxes in freshwater
400 ecosystems. In events of mass zooplankton mortality, the water column can be loaded with a
401 considerable amount of carcass-derived LOM. By decreasing the bacterial diversity and
402 selecting specialized bacteria, zooplankton carcasses potentially have further and so far likely
403 unknown consequences on microbial dynamics and carbon fluxes. Indeed, our results suggest
404 that a significant part of zooplankton carcasses is respired by bacteria. Therefore, our study
405 provides evidence that quantifying the implication of zooplankton carcasses in the functioning
406 of aquatic ecosystems is of primordial importance to understand the amount of carbon
407 produced in and released from freshwaters.

408 **Experimental Procedures**

409 **Experimental setup**

410 The experiment was conducted in laboratory microcosms, which were set up in 1L
411 acid-washed and muffled (4h, 450 °C) glass bottles half-filled with artificial lake water. The
412 microcosms were inoculated with a concentrated bacterial community from the acidic bog
413 lake Grosse Fuchskuhle (Northeastern Germany, 53°06'N 12°59'E; more detailed information
414 is provided in the Supplementary Methods). Microcosms were sealed with PTFE-coated
415 silicone septa, placed on a roller apparatus (Wheaton, USA), and incubated for 15 days in the
416 dark at 20°C. The duration of the experiment, irradiance, temperature, and the rolling mode
417 were chosen to fall within the range of natural conditions of sinking zooplankton carcasses in
418 a water column (Tang *et al.*, 2009, 2014).

419 One set of microcosms (**HD**) was amended with humic matter and ^{13}C-labeled
420 *Daphnia* carcasses (Fig. S1). The detailed description of the amendments including their
421 preparation is available in the Supplementary Methods. Carcasses control microcosms (**D**)
422 were amended solely with ^{13}C-labeled *Daphnia* carcasses in the same quantity and from the
423 same batch of *Daphnia* as in **HD** microcosms. Humic matter control microcosms (**H**) were
424 amended with humic matter only in the same quantity as in **HD** microcosms (Fig. S1).
425 Further, blank microcosms (**B**) with no added organic matter were included to determine
426 whether the bacterial community was capable of growing without the extra addition of
427 organic carbon (Fig. S1). Each experimental treatment was conducted in five replicates.

428 **Bacterial counts and community composition**

429 Microbial abundances were determined after filtration of 5 mL of water through
430 Nucleopore track-etched membrane filters with a pore size of 0.2 µm (Whatman, UK). Then,
431 samples were stained with 4',6-diamidino-2-phenylindole (DAPI) to monitor cell numbers
432 using an imaging system linked to a Leica epifluorescence microscope. Pictures were taken
433 from 30-50 fields and abundances were determined using the CellC software (Tampere
434 University of Technology, Finland, https://sites.google.com/site/cellcsoftware/).
435 For DNA extraction, 150 mL of water was filtered through 0.22 µm GVWP filters
436 (Millipore, Germany) and total DNA was extracted according to a modified protocol
437 described by Nercessian *et al.* (2005) (see Supplementary Methods for details). DNA
438 concentrations were determined with a Quantus fluorometer (Promega, USA), following the
439 manufacturer's instructions. PCR, library preparation and sequencing was done by LGC
440 Genomics (Berlin, Germany). Briefly, the V3-V4 region was amplified using primers 341F-
441 785R (Klindworth *et al.*, 2013), followed by library preparation (2x300 bp) and sequencing
442 on a MiSeq Illumina platform. Sequences were quality checked and analyzed using Mothur
443 v1.37.6 (Schloss *et al.*, 2009), see Supplementary Methods for the detailed workflow. The

444 sequence data was deposited in Genbank under the following accession number:
445 PRJNA418906.

446 **Organic carbon concentration and composition**

447 Directly after sampling, water was passed through pre-combusted (4 h, 450°C) GF75
448 filters (Advantec, nominal pore size of 0.3 µm). Particulate organic carbon (POC) collected
449 on the filters was measured with an Eltra SC 800 (Eltra, Germany). One subsample of filtrate
450 was processed directly to measure the DOC concentration with a TOC-V_{CPH} (Shimadzu,
451 Kyoto, Japan) as well as the phosphate concentration using a FIAstar 5000 (Foss, USA). Total
452 organic carbon (TOC) concentration was estimated by summing up the DOC and POC
453 concentrations.

454 Another subsample of filtrate was stored at 4°C for three weeks prior analysis with
455 liquid chromatography - organic carbon detection – organic nitrogen detection (LC-OCD-
456 OND, DOC Labor, Germany). The LC-OCD-OND allows distinguishing between HMWS,
457 LMWS, and humic substances (Huber *et al.*, 2011). Nevertheless, its sensitivity is not
458 sufficient for analyzing samples with low DOC concentration (<0.2 mg L^{-1}). That was the
459 case for the D and B microcosms which were therefore not analyzed by LC-OCD-OND.

460 **Spectral characteristics of DOM**

461 DOM optical characteristics were obtained with a UV-Vis spectrophotometer (Hitachi
462 U2900, Germany) and a spectrofluorometer (Hitachi F7000, Germany). Absorbance spectra
463 were recorded from 190 to 800 nm with an increment of 1 nm and used to compute the
464 specific ultraviolet absorbance at 254 nm ($SUVA_{254}$) and absorption spectral slopes (Weishaar
465 *et al.*, 2003; Helms *et al.*, 2008). $SUVA_{254}$ is an indicator of aromaticity and chemical
466 reactivity while the absorption slopes are used as proxies for DOM molecular weight.

467 Excitation emission matrices (EEMs) were generated with excitation wavelengths
468 ranging from 220 to 450 nm and emission wavelengths ranging from 230 to 600 nm, both
469 with 5 nm increments. EEMs were corrected with a MilliQ water sample and for inner filter
470 effect using the absorbance-based method (Christmann *et al.*, 1980; Murphy *et al.*, 2013).
471 Then, fluorescence, humification and freshness indices, as well as specific fluorescence
472 intensity at various peaks were calculated as described by Hansen *et al.* (2016).

473 **Carbon stable isotope ratio**

474 Stable isotope analysis of the respired CO_2 provides information on carbon substrates
475 metabolized by the microbial community (Fabian *et al.*, 2017). The ratio of $^{13}C/^{12}C$ in the
476 dissolved CO_2 was measured directly in each microcosm by a membrane-inlet mass-
477 spectrometer dissolved gas analyzer (HiCube pumping station, Pfeiffer Vacuum and Bay
478 Instruments membrane, USA), controlled by Quickdata software. The sampling capillary was
479 inserted through the PTFE-coated silicone septa prior to opening microcosms in order to
480 avoid gas leakages. Concentrations of $^{12}CO_2$ and $^{13}CO_2$ were obtained from the ion currents
481 sequentially recorded at mass to charge (m/z) ratios of 44 and 45, respectively.

482 For the carbon stable isotope ratio in POC and DOC, 100 ml of water was passed
483 through GF75 filters (Advantec, USA) and both the flow-through and the filter (all five
484 replicates were pooled onto one filter to have enough material for subsequent analyzes) were
485 collected and freeze-dried. Moreover, we dried 1 mg of acid-killed *Daphnia* and
486 approximately 1 mg of extracted humic matter for carbon stable isotope ratio analysis. The
487 samples were analyzed with an Elemental Analyzer (Thermo Flash EA 2000), coupled to a
488 continuous-flow isotope ratio mass spectrometer (Thermo Finnigan Delta V) via an open split
489 interface (Thermo Finnigan Conflow IV) in the IRMS Laboratory of the Leibniz Institute for
490 Baltic Sea Research Warnemünde (Germany), and with a PDZ Europa ANCA-GSL elemental

analyzer interfaced to a PDZ Europa 20-20 isotope ratio mass spectrometer (Sercon Ltd., Cheshire, UK) at the UC Davis Stable Isotope Facility (USA).

Decomposition calculations

To test for a possible priming effect, we used an addition model as in Hannides and Aller (2016). Initial and final total organic carbon concentrations in the humic control, i.e. TOC_i (H) and TOC_f (H), respectively, in the carcass control, i.e. TOC_i (D) and TOC_f (D), and in the blank, i.e. TOC_i (B) and TOC_f (B), respectively, were used to predict the degradation of total organic carbon (ΔTOC) in the **HD** microcosm. Thereby, we assumed that the degradation rates of carbon sources observed in the control microcosms are conserved when humic matter and carcasses are incubated together. The predicted ΔTOC(H+D) was compared with the measured ΔTOC(HD) to detect any enhanced degradation of organic carbon caused by a potential "priming effect". Similarly, data on CO_2 concentration and isotope ratio ($^{13}CO_2/^{12}CO_2$) in the microcosms was used to calculate respiration of recalcitrant and labile carbon pools. We assumed that if a priming effect is present, there should be a difference in the observed isotope ratio between measured and predicted CO_2, based on the sum of control values.

The carcass carbon fraction (F_c) in DOC, POC and CO_2 was calculated via a stable isotope mixing model (Hopkins and Ferguson, 2012). We also applied Keeling plot analyses of dissolved CO_2 (Pataki *et al.*, 2003) to estimate the $\delta^{13}C$ of the carbon source respired in the respective microcosms. Descriptive calculation formulas are available in the Supplementary Methods.

Statistical analyses

For alpha-diversity calculations of bacterial communities, individual samples were rarefied to the lowest number of reads in a sample (10080), with 10 iterations per sample

515 using QIIME (Caporaso *et al.*, 2010). Shannon biodiversity index was calculated to estimate
516 richness and evenness of the microcosm communities. Beta-diversity of bacterial
517 communities was calculated by using the Bray-Curtis similarity coefficients (Bray and Curtis,
518 1957) using QIIME.

519 All analyses described below were run via R version 3.3.3 (R Development Core
520 Team, 2006). R package *vegan* (vegan: Community Ecology Package, 2017, https://CRAN.R-
521 project.org/package=vegan) was used to carry out principal coordinate analysis (PCoA) and to
522 calculate ANOSIM and SIMPER (Clarke, 1993).

523 Bacterial community composition was linked to DOC characteristics which
524 significantly differentiated microcosms. We used the least absolute shrinkage and selection
525 operator (LASSO) to select genera that were influenced by a variation in DOM composition
526 (Traving *et al.*, 2016). Before designing the LASSO models, we summed the abundances of
527 OTUs belonging to the same genus and performed a centered log-ratio transformation (Gloor
528 and Reid, 2016) of the absolute abundances of all genera. To visualize the outcome, we
529 depicted the selected genera in two different networks using Cytoscape software (Shannon *et*
530 *al.*, 2003).

531 All differences between treatments were tested using a one-way analysis of variance
532 (ANOVA) and post-hoc Tukey tests. Pairwise comparisons between initial and final
533 parameters of microcosms and between two treatments were done using Student's t-test and
534 Wilcoxon rank sum test. Normality was checked by Shapiro–Wilks tests when necessary.

535 **Acknowledgements**

536 This research was funded by German Science Foundation (GR 1540/29-1,
537 GR1549/23-1) and the Russian Foundation for Basic Research (No. 16-54-12048), and partly
538 supported by Russian Federal Tasks of Fundamental Research (project No. 51.1.1) and by the
539 Council on grants from the President of the Russian Federation for support of Leading

Scientific Schools (grant NSh-9249.2016.5). OVK was supported by Michail-Lomonosov-Programme-Linie A, 2015 (57180771) funded by the Ministry of Education and Science of the Russian Federation and the German Academic Exchange Service (DAAD). The authors thank Uta Mallok for DOC and phosphate concentration measurements. We are grateful to Maren Voss and Iris Liskow in the IRMS Laboratory of the Leibniz Institute for Baltic Sea Research Warnemünde (Germany) for stable isotope analysis. We greatly appreciate the useful advices of Jenny Fabian and Isabell Klawonn on stable isotope sample preparation and data handling. We thank two anonymous reviewers for carefully reading the manuscript and suggesting substantial improvements.

The authors declare no conflict of interests.

References

Adams, H.E., Crump, B.C., and Kling, G.W. (2010) Temperature controls on aquatic bacterial production and community dynamics in arctic lakes and streams. *Environ Microbiol* **12**: 1319–1333.

Amado, A.M., Cotner, J.B., Cory, R.M., Edhlund, B.L., and McNeill, K. (2015) Disentangling the interactions between photochemical and bacterial degradation of dissolved organic matter: amino acids play a central role. *Microb Ecol* **69**: 554–566.

Attermeyer, K., Hornick, T., Kayler, Z.E., Bahr, A., Zwirnmann, E., Grossart, H.-P., and Premke, K. (2014) Enhanced bacterial decomposition with increasing addition of autochthonous to allochthonous carbon without any effect on bacterial community composition. *Biogeosciences* **11**: 1479–1489.

Attermeyer, K., Tittel, J., Allgaier, M., Frindte, K., Wurzbacher, C., Hilt, S., et al. (2015) Effects of light and autochthonous carbon additions on microbial turnover of allochthonous organic carbon and community composition. *Microb Ecol* **69**: 361–371.

Battin, T.J., Luyssaert, S., Kaplan, L.A., Aufdenkampe, A.K., Richter, A., and Tranvik, L.J. (2009) The boundless carbon cycle. *Nat Geosci* **2**: 598–600.

Bell, K.S., Philp, J.C., Aw, D.W.J., and Christofi, N. (1998) The genus *Rhodococcus*. *J Appl Microbiol* **85**: 195–210.

Bengtsson, M.M., Wagner, K., Burns, N.R., Herberg, E.R., Wanek, W., Kaplan, L.A., and Battin, T.J. (2014) No evidence of aquatic priming effects in hyporheic zone microcosms. *Sci Rep* **4**: 5187.

Bianchi, T.S. (2011) The role of terrestrially derived organic carbon in the coastal ocean: A changing paradigm and the priming effect. *Proc Natl Acad Sci* **108**: 19473–19481.

Bianchi, T.S., Thornton, D.C.O., Yvon-Lewis, S.A., King, G.M., Eglinton, T.I., Shields, M.R., et al. (2015) Positive priming of terrestrially derived dissolved organic matter in a freshwater microcosm system. *Geophys Res Lett* **42**: 5460–5467.

Bickel, S.L., and Tang, K.W. (2010) Microbial decomposition of proteins and lipids in copepod versus rotifer carcasses. *Mar Biol* **157**: 1613–1624.

Blanchet, M., Pringault, O., Bouvy, M., Catala, P., Oriol, L., Caparros, J., et al. (2015) Changes in bacterial community metabolism and composition during the degradation of dissolved organic matter from the jellyfish *Aurelia aurita* in a Mediterranean coastal lagoon. *Environ Sci Pollut Res* **22**: 13638–13653.

Blanchet, M., Pringault, O., Panagiotopoulos, C., Lefevre, D., Charriere, B., Ghiglione, J.-F., et al. (2017) When riverine dissolved organic matter (DOM) meets labile DOM in coastal waters: changes in bacterial community activity and composition. *Aquat Sci* **79**: 27–43.

Bray, J.R., and Curtis, J.T. (1957) An ordination of the upland forest communities of Southern Wisconsin. *Ecol Monogr* **27**: 325–349.

Caporaso, J.G., Kuczynski, J., Stombaugh, J., Bittinger, K., Bushman, F.D., Costello, E.K., et al. (2010) QIIME allows analysis of high-throughput community sequencing data. *Nat Methods* **7**: 335–336.

Catalán, N., Kellerman, A.M., Peter, H., Carmona, F., and Tranvik, L.J. (2015) Absence of a priming effect on dissolved organic carbon degradation in lake water. *Limnol Oceanogr* **60**: 159–168.

Christmann, D.R., Crouch, S.R., Holland, J.F., and Timnick, A. (1980) Correction of right-angle molecular fluorescence measurements for absorption of fluorescence radiation. *Anal Chem* **52**: 291–295.

Clarke, K.R. (1993) Non-parametric multivariate analyses of changes in community structure. *Austral Ecol* **18**: 117–143.

Dorado-García, I., Syväranta, J., Devlin, S.P., Medina-Sánchez, J.M., and Jones, R.I. (2015) Experimental assessment of a possible microbial priming effect in a humic boreal lake. *Aquat Sci* 1–12.

Doronina, N., Kaparullina, E., and Trotsenko, Y. (2014) The Family Methylophilaceae. In Rosenberg, E., DeLong, E.F., Lory, S., Stackebrandt, E., and Thompson, F. (eds), *The Prokaryotes: Alphaproteobacteria and Betaproteobacteria*. Springer Berlin Heidelberg, Berlin, Heidelberg, pp. 869–880.

Dubovskaya, O.P., Gladyshev, M.I., Gubanov, V.G., and Makhutova, O.N. (2003) Study of non-consumptive mortality of Crustacean zooplankton in a Siberian reservoir using staining for live/dead sorting and sediment traps. *Hydrobiologia* **504**: 223–227.

Dubovskaya, O.P., Tolomeev, A.P., Kirillin, G., Buseva, Z., Tang, K.W., and Gladyshev, M.I. (2018) Effects of water column processes on the use of sediment traps to measure zooplankton non-predatory mortality: a mathematical and empirical assessment. *J Plankton Res* **40**: 91–106.

613 Elliott, D.T., Harris, C.K., and Tang, K.W. (2010) Dead in the water: The fate of copepod
614 carcasses in the York River estuary, Virginia. *Limnol Oceanogr* **55**: 1821–1834.
615 Evtushenko, L.I. (2015) *Marmoricola*. In *Bergey's Manual of Systematics of Archaea and*
616 *Bacteria*. John Wiley & Sons, Ltd.
617 Fabian, J., Zlatanovic, S., Mutz, M., and Premke, K. (2017) Fungal–bacterial dynamics and
618 their contribution to terrigenous carbon turnover in relation to organic matter quality.
619 *ISME J* **11**: 415–425.
620 Fonte, E.S., Amado, A.M., Meirelles-Pereira, F., Esteves, F.A., Rosado, A.S., and Farjalla,
621 V.F. (2013) The combination of different carbon sources enhances bacterial growth
622 efficiency in aquatic ecosystems. *Microb Ecol* **66**: 871–878.
623 Gloor, G.B., and Reid, G. (2016) Compositional analysis: a valid approach to analyze
624 microbiome high-throughput sequencing data. *Can J Microbiol* **62**: 692–703.
625 Glud, R.N., Grossart, H.-P., Larsen, M., Tang, K.W., Arendt, K.E., Rysgaard, S., et al. (2015)
626 Copepod carcasses as microbial hot spots for pelagic denitrification. *Limnol Oceanogr*
627 **60**: 2026–2036.
628 Gómez-Consarnau, L., Lindh, M.V., Gasol, J.M., and Pinhassi, J. (2012) Structuring of
629 bacterioplankton communities by specific dissolved organic carbon compounds.
630 *Environ Microbiol* **14**: 2361–2378.
631 Gontikaki, E., Thornton, B., Huvenne, V.A.I., and Witte, U. (2013) Negative priming effect
632 on organic matter mineralisation in NE Atlantic slope sediments. *PLoS ONE* **8**:
633 e67722.
634 Gontikaki, E., Thornton, B., Cornulier, T., and Witte, U. (2015) Occurrence of priming in the
635 degradation of lignocellulose in marine sediments. *PLoS ONE* **10**: e0143917.
636 Goto, M. (2015) *Rhizobacter.* In, *Bergey's Manual of Systematics of Archaea and Bacteria*.
637 John Wiley & Sons, Ltd.

Grinhut, T., Hadar, Y., and Chen, Y. (2007) Degradation and transformation of humic substances by saprotrophic fungi: processes and mechanisms. *Fungal Biol Rev.* 21: 179–189.

Grossart, H.-P. (2010) Ecological consequences of bacterioplankton lifestyles: changes in concepts are needed. *Environ Microbiol Rep* **2**: 706–714.

Grossart, H.-P. and Rojas-Jimenez, K. (2016) Aquatic fungi: targeting the forgotten in microbial ecology. *Curr Opin Microbiol* **31**: 140–145.

Grossart, H.-P., Tang, K.W., Kiørboe, T., and Ploug, H. (2007) Comparison of cell-specific activity between free-living and attached bacteria using isolates and natural assemblages. *FEMS Microbiol Lett* **266**: 194–200.

Grossart, H.-P., Jezbera, J., Hornak, K., Hutalle, K.M.L., Buck, U., and Simek, K. (2008) Top-down and bottom-up induced shifts in bacterial abundance, production and community composition in an experimentally divided humic lake. *Environ Microbiol* **10**: 635–652.

Guenet, B., Danger, M., Harrault, L., Allard, B., Jauset-Alcala, M., Bardoux, G., et al. (2013) Fast mineralization of land-born C in inland waters: first experimental evidences of aquatic priming effect. *Hydrobiologia* **721**: 35–44.

Hannides, A.K. and Aller, R.C. (2016) Priming effect of benthic gastropod mucus on sedimentary organic matter remineralization. *Limnol Oceanogr* **61**: 1640–1650.

Hansen, A.M., Kraus, T.E.C., Pellerin, B.A., Fleck, J.A., Downing, B.D., and Bergamaschi, B.A. (2016) Optical properties of dissolved organic matter (DOM): Effects of biological and photolytic degradation. *Limnol Oceanogr* **61**: 1015–1032.

Heathcote, A., Filstrup, C., Kendall, D., and Downing, J. (2016) Biomass pyramids in lake plankton: influence of Cyanobacteria size and abundance. *Inland Waters* **6**: 250-257.

Helms, J.R., Stubbins, A., Ritchie, J.D., Minor, E.C., Kieber, D.J., and Mopper, K. (2008) Absorption spectral slopes and slope ratios as indicators of molecular weight, source,

and photobleaching of chromophoric dissolved organic matter. *Limnol Oceanogr* **53**: 955–969.

Henson, M.W., Hanssen, J., Spooner, G., Flemming, P., Pukonen, M., Stahr, F., and Thrash, J.C. (2016) Microbial regime changes and indicators of eutrophication on the Mississippi River identified via a human-powered 2900 km transect. *bioRxiv*. doi: https://doi.org/10.1101/091512

Hoikkala, L., Tammert, H., Lignell, R., Eronen-Rasimus, E., Spilling, K., and Kisand, V. (2016) Autochthonous dissolved organic matter drives bacterial community composition during a bloom of filamentous Cyanobacteria. *Front Mar Sci* **3**: 111.

Hopkins, J.B. and Ferguson, J.M. (2012) Estimating the diets of animals using stable isotopes and a comprehensive Bayesian mixing model. *PLoS ONE* **7**: e28478.

Hotchkiss, E.R., Hall, R.O., Baker, M.A., Rosi-Marshall, E.J., and Tank, J.L. (2014) Modeling priming effects on microbial consumption of dissolved organic carbon in rivers. *J Geophys Res Biogeosciences* **119**: 982–995.

Huber, S.A., Balz, A., Abert, M., and Pronk, W. (2011) Characterisation of aquatic humic and non-humic matter with size-exclusion chromatography-organic carbon detection-organic nitrogen detection (LC-OCD-OND). *Water Res* **45**: 879–885.

Hutalle-Schmelzer, K.M.L., Zwirnmann, E., Krüger, A., and Grossart, H.-P. (2010) Enrichment and cultivation of pelagic bacteria from a humic lake using phenol and humic matter additions. *FEMS Microbiol Ecol* **72**: 58–73.

Johansen, J.E., Binnerup, S.J., Kroer, N., and Mølbak, L. (2005) *Luteibacter rhizovicinus gen. nov.*, *sp. nov.*, a yellow-pigmented gammaproteobacterium isolated from the rhizosphere of barley (*Hordeum vulgare* L.). *Int J Syst Evol Microbiol* **55**: 2285–2291.

Kämpfer, P. (2015) *Sphingobacteriales ord. nov.* In *Bergey's Manual of Systematics of Archaea and Bacteria*. John Wiley & Sons, Ltd.

689 Kirillin, G., Grossart, H.-P., and Tang, K.W. (2012) Modeling sinking rate of zooplankton
690 carcasses: Effects of stratification and mixing. *Limnol Oceanogr* **57**: 881–894.
691 Kisand, V., Gebhardt, S., Rullkötter, J., and Simon, M. (2013) Significant bacterial
692 transformation of riverine humic matter detected by pyrolysis GC–MS in serial
693 chemostat experiments. *Mar Chem* **149**: 23–31.
694 Klindworth, A., Pruesse, E., Schweer, T., Peplies, J., Quast, C., Horn, M., and Glöckner, F.O.
695 (2013) Evaluation of general 16S ribosomal RNA gene PCR primers for classical and
696 next-generation sequencing-based diversity studies. *Nucleic Acids Res* **41**: e1.
697 Kuehn, K.A., Francoeur, S.N., Findlay, R.H., and Neely, R.K. (2014) Priming in the
698 microbial landscape: periphytic algal stimulation of litter-associated microbial
699 decomposers. *Ecology* **95**: 749–762.
700 Kuykendall, L.D. (2005) Order VI. *Rhizobiales ord. nov*. In, *Bergey's Manual of Systematics*
701 *of Archaea and Bacteria*. John Wiley & Sons, Ltd.
702 Landa, M., Blain, S., Christaki, U., Monchy, S., and Obernosterer, I. (2016) Shifts in bacterial
703 community composition associated with increased carbon cycling in a mosaic of
704 phytoplankton blooms. *ISME J* **10**: 39–50.
705 Lindh, M.V., Lefébure, R., Degerman, R., Lundin, D., Andersson, A., and Pinhassi, J. (2015)
706 Consequences of increased terrestrial dissolved organic matter and temperature on
707 bacterioplankton community composition during a Baltic Sea mesocosm experiment.
708 *AMBIO* **44**: 402–412.
709 McBride, M.J. (2014) The Family *Flavobacteriaceae*. In Rosenberg, E., DeLong, E.F., Lory,
710 S., Stackebrandt, E., and Thompson, F. (eds), *The Prokaryotes: other major lineages*
711 *of Bacteria and the Archaea*. Springer Berlin Heidelberg, Berlin, Heidelberg, pp. 643–
712 676.

713 Meziti, A., Kormas, K.A., Moustaka-Gouni, M., and Karayanni, H. (2015) Spatially uniform
714 but temporally variable bacterioplankton in a semi-enclosed coastal area. *Syst Appl*
715 *Microbiol* **38**: 358–367.
716 Murphy, K.R., Stedmon, C.S., Graeber, D., and Bro, R. (2013) Fluorescence spectroscopy and
717 multi-way techniques. PARAFAC. *Anal Methods* **5**: 6557–6566.
718 Nercessian, O., Noyes, E., Kalyuzhnaya, M.G., Lidstrom, M.E., and Chistoserdova, L. (2005)
719 Bacterial populations active in metabolism of C1 compounds in the sediment of Lake
720 Washington, a freshwater lake. *Appl Environ Microbiol* **71**: 6885–6899.
721 Newton, R.J., Jones, S.E., Eiler, A., McMahon, K.D., and Bertilsson, S. (2011) A guide to the
722 natural history of freshwater lake bacteria. *Microbiol Mol Biol Rev* **75**: 14–49.
723 van Nugteren, P., Moodley, L., Brummer, G.-J., Heip, C.H.R., Herman, P.M.J., and
724 Middelburg, J.J. (2009) Seafloor ecosystem functioning: the importance of organic
725 matter priming. *Mar Biol* **156**: 2277–2287.
726 O'Sullivan, L.A., Rinna, J., Humphreys, G., Weightman, A.J., and Fry, J.C. (2005) *Fluviicola*
727 *taffensis gen. nov., sp. nov*., a novel freshwater bacterium of the family
728 *Cryomorphaceae* in the phylum '*Bacteroidetes*'. *Int J Syst Evol Microbiol* **55**: 2189–
729 2194.
730 Pace, M.L., Cole, J.J., Carpenter, S.R., Kitchell, J.F., Hodgson, J.R., Van de Bogert, M.C., et
731 al. (2004) Whole-lake carbon-13 additions reveal terrestrial support of aquatic food
732 webs. *Nature* **427**: 240–243.
733 Pataki, D.E., Ehleringer, J.R., Flanagan, L.B., Yakir, D., Bowling, D.R., Still, C.J., et al.
734 (2003) The application and interpretation of Keeling plots in terrestrial carbon cycle
735 research. *Glob Biogeochem Cycles* **17**: 1022.
736 Rocker, D., Kisand, V., Scholz-Böttcher, B., Kneib, T., Lemke, A., Rullkötter, J., and Simon,
737 M. (2012a) Differential decomposition of humic acids by marine and estuarine
738 bacterial communities at varying salinities. *Biogeochemistry* **111**: 331–346.

739 Rocker, D., Brinkhoff, T., Grüner, N., Dogs, M., and Simon, M. (2012b) Composition of
740 humic acid-degrading estuarine and marine bacterial communities. *FEMS Microbiol*
741 *Ecol* **80**: 45–63.
742 Rojas-Jimenez, K., Fonvielle, J.A., Ma, H., and Grossart, H.-P. (2017) Transformation of
743 humic substances by the freshwater Ascomycete Cladosporium sp. *Limnol Oceanogr*
744 **62**: 1955-1962.
745 Schloss, P.D., Westcott, S.L., Ryabin, T., Hall, J.R., Hartmann, M., Hollister, E.B., et al.
746 (2009) Introducing mothur: open-source, platform-independent, community-supported
747 software for describing and comparing microbial communities. *Appl Environ*
748 *Microbiol* **75**: 7537–7541.
749 Schmidt, M.W.I., Torn, M.S., Abiven, S., Dittmar, T., Guggenberger, G., Janssens, I.A., et al.
750 (2011) Persistence of soil organic matter as an ecosystem property. *Nature* **478**: 49–
751 56.
752 Segers, P., Vancanneyt, M., Pot, B., Torck, U., Hoste, B., Dewettinck, D., et al. (1994)
753 Classification of *Pseudomonas diminuta* Leifson and Hugh 1954 and *Pseudomonas*
754 *vesicularis* Busing, Doll, and Freytag 1953 in *Brevundimonas gen. nov.* as
755 *Brevundimonas diminuta comb. nov.* and *Brevundimonas vesicularis comb. nov.*,
756 respectively.
757 Shannon, P., Markiel, A., Ozier, O., Baliga, N.S., Wang, J.T., Ramage, D., et al. (2003)
758 Cytoscape: a software environment for integrated models of biomolecular interaction
759 networks. *Genome Res* **13**: 2498–2504.
760 Shoemaker, K.M. and Moisander, P.H. (2015) Microbial diversity associated with copepods
761 in the North Atlantic subtropical gyre. *FEMS Microbiol Ecol* **91**: fiv064-fiv064.
762 Song, J., Choo, Y.-J., and Cho, J.-C. (2008) *Perlucidibaca piscinae gen. nov., sp. nov.*, a
763 freshwater bacterium belonging to the family *Moraxellaceae. Int J Syst Evol*
764 *Microbiol* **58**: 97–102.

Spencer, R.G.M., Aiken, G.R., Butler, K.D., Dornblaser, M.M., Striegl, R.G., and Hernes, P.J. (2009) Utilizing chromophoric dissolved organic matter measurements to derive export and reactivity of dissolved organic carbon exported to the Arctic Ocean: A case study of the Yukon River, Alaska. *Geophys Res Lett* **36**: L06401, doi: 10.1029/2008GL036831 .

Steen, A.D., Quigley, L.N.M., and Buchan, A. (2015) Evidence for the priming effect in a planktonic estuarine microbial community. *Front Mar Sci* **3**: 6.

Steinberg, D.K. and Landry, M.R. (2017) Zooplankton and the ocean carbon cycle. *Annu Rev Mar Sci* **9**: 413–444.

Stubbins, A., Spencer, R.G.M., Chen, H., Hatcher, P.G., Mopper, K., Hernes, P.J., et al. (2010) Illuminated darkness: Molecular signatures of Congo River dissolved organic matter and its photochemical alteration as revealed by ultrahigh precision mass spectrometry. *Limnol Oceanogr* **55**: 1467–1477.

Tang, K.W., Hutalle, K.M.L., and Grossart, H. (2006) Microbial abundance, composition and enzymatic activity during decomposition of copepod carcasses. *Aquat Microb Ecol* **45**: 219–227.

Tang, K., Dziallas, C., Hutalle-Schmelzer, K., and Grossart, H.-P. (2009) Effects of food on bacterial community composition associated with the copepod *Acartia tonsa* Dana. *Biol Lett* **5**: 549.

Tang, K.W., Turk, V., and Grossart, H. (2010) Linkage between crustacean zooplankton and aquatic bacteria. *Aquat Microb Ecol* **61**: 261–277.

Tang, K.W., Gladyshev, M.I., Dubovskaya, O.P., Kirillin, G., and Grossart, H.-P. (2014) Zooplankton carcasses and non-predatory mortality in freshwater and inland sea environments. *J Plankton Res* **36**: 597–612.

Tranvik, L.J. and Kokalj, S. (1998) Decreased biodegradability of algal DOC due to interactive effects of UV radiation and humic matter. *Aquat Microb Ecol* **14**: 301–307.

Tranvik, L.J., Downing, J.A., Cotner, J.B., Loiselle, S.A., Striegl, R.G., Ballatore, T.J., et al. (2009) Lakes and reservoirs as regulators of carbon cycling and climate. *Limnol Oceanogr* **54**: 2298–2314.

Traving, S.J., Bentzon-Tilia, M., Knudsen-Leerbeck, H., Mantikci, M., Hansen, J.L.S., Stedmon, C.A., et al. (2016) Coupling bacterioplankton populations and environment to community function in coastal temperate waters. *Front Microbiol* **7**: 1533.

Trusova, M.Y., Kolmakova, O.V., and Gladyshev, M.I. (2012) Seasonal features of consumption of lysine by uncultivated bacterial plankton of eutrophic water reservoir. *Contemp Probl Ecol* **5**: 391–398.

Vachon, D., Prairie, Y.T., Guillemette, F., and del Giorgio, P.A. (2017) Modeling allochthonous dissolved organic carbon mineralization under variable hydrologic regimes in boreal lakes. *Ecosystems* **20**: 781–795.

Ward, N.D., Keil, R.G., Medeiros, P.M., Brito, D.C., Cunha, A.C., Dittmar, T., et al. (2013) Degradation of terrestrially derived macromolecules in the Amazon River. *Nat Geosci* **6**: 530–533.

Weishaar, J.L., Aiken, G.R., Bergamaschi, B.A., Fram, M.S., Fujii, R., and Mopper, K. (2003) Evaluation of specific ultraviolet absorbance as an indicator of the chemical composition and reactivity of dissolved organic carbon. *Environ Sci Technol* **37**: 4702–4708.

Table and Figure legends

Table 1. Chemical and optical parameters of experimental microcosms varying in carbon sources: $\mathbf{B_i}$ – blank initial, $\mathbf{B_f}$ – blank final, $\mathbf{H_i}$ – humic matter initial, $\mathbf{H_f}$ – humic matter final, $\mathbf{D_i}$ – carcasses initial, $\mathbf{D_f}$ – carcasses final, $\mathbf{HD_i}$ – humic matter + carcasses initial, $\mathbf{HD_f}$ – humic matter + carcasses final. Parameters in $\mathbf{D_i}$ and $\mathbf{HD_i}$ were not measured directly but calculated from parameters in $\mathbf{B_i}$ and $\mathbf{H_i}$. Values are given as means of five replicates ±

standard errors, except for the initial DNA concentration values obtained from a single measurement. nd = not determined.

Table 2. Alpha-diversity of bacterial communities in the microcosms with additions of humic matter (**H**), *Daphnia* carcasses (**D**), humic matter and carcasses together (**HD**), and blank with no carbon sources (**B**). Values are given as means of five replicates ± standard errors, except for the initial inoculate (**I**) obtained from a single measurement, and **B** microcosms (four replicates due to too low DNA content in one sample).

Table 3. Abundances (in %) of the quantitatively prominent OTUs contributing the most to the dissimilarity among the inoculum sample (**I**) and the end points of the microcosms with additions of humic matter (**H**), *Daphnia* carcasses (**D**), humic matter and carcasses together (**HD**), and blank with no carbon sources (**B**). Values are given as means of five replicates ± standard errors, except for the inoculum sample obtained from a single measurement, and **B** microcosms (four replicates due to low DNA content of two samples which were pooled).

Fig. 1 Relative abundance of major bacterial phyla and classes of Proteobacteria in the initial sample (**I**) and the end points of microcosms with additions of humic matter (**H**), *Daphnia* carcasses (**D**), humic matter and carcasses together (**HD**), and blank with no carbon sources (**B**).

Fig. 2 Principal coordinate analysis of the initial sample (I) and the end points of microcosms with additions of humic matter (**H**), *Daphnia* carcasses (**D**), humic matter and carcasses together (**HD**), and blank with no carbon sources (**B**), based on Bray-Curtis community similarity, calculated as relative abundance of operational taxonomic units (OTUs).

Fig. 3 Carbon fractions originated from *Daphnia* carcasses at the end of the experiment in pools of dissolved (DOC) and particulate organic carbon (POC) as well as in

841 dissolved CO_2 in microcosms with humic matter and *Daphnia* carcasses (**HD**) and carcasses
842 only (**D**). The area size of diagrams is relative to carbon concentration.

843 **Fig. 4** Network of bacterial genera connected with major DOM parameters,
844 significantly different in pairs of microcosms: a – microcosms **H** – humic matter, and **D** –
845 carcasses; b – microcosms **HD** – humic matter + carcasses, and **D** – carcasses. Nodes that
846 interact positively are connected by solid black edges, nodes connected by dashed edges have
847 negative interactions. Legend: DOC – concentration of DOC; HIX – humification index, FIX
848 – fluorescence index, fresh – freshness index, SUVA254 – Specific UV absorbance at 254
849 nm, A/T – ratio between the specific fluorescence at peak A (excitation 240-260 nm/emission
850 400-500 nm, UVC humic-like fluorescent component) and peak T (excitation 270-285
851 nm/emission 340-380 nm, tryptophan-like fluorescent component).

Table 1. Chemical and optical parameters of experimental microcosms varying in carbon sources: $\mathbf{B_i}$ – blank initial, $\mathbf{B_f}$ – blank final, $\mathbf{H_i}$ – humic matter initial, $\mathbf{H_f}$ – humic matter final, $\mathbf{D_i}$ – carcasses initial, $\mathbf{D_f}$ – carcasses final, $\mathbf{HD_i}$ – humic matter + carcasses initial, $\mathbf{HD_f}$ – humic matter + carcasses final. Parameters in $\mathbf{D_i}$ and $\mathbf{HD_i}$ were not measured directly but calculated from parameters in $\mathbf{B_i}$ and $\mathbf{H_i}$. Values are given as means of five replicates ± standard errors, except for the initial DNA concentration values obtained from a single measurement. nd = not determined.

Chemical parameters	$\mathbf{B_i}$	$\mathbf{B_f}$	$\mathbf{H_i}$	$\mathbf{H_f}$	$\mathbf{D_i}$	$\mathbf{D_f}$	$\mathbf{HD_i}$	$\mathbf{HD_f}$
DOC $mg \cdot L^{-1}$	0.221 ± 0.003	0.216 ± 0.009	3.025 ± 0.070	2.952 ± 0.109	0.221 ± 0.003	0.269 ± 0.016	3.025 ± 0.070	2.944 ± 0.017
POC $mg \cdot L^{-1}$	0.044 ± 0.006	0.028 ± 0.004	0.033 ± 0.002	0.067 ± 0.010	1.378 ± 0.044	0.333 ± 0.015	1.367 ± 0.040	0.354 ± 0.007
Humic substances ($mg \cdot L^{-1}$)	nd	nd	2.065 ± 0.034	2.130 ± 0.015	nd	nd	2.065 ± 0.034	2.125 ± 0.009
Building blocks of humic substances ($mg \cdot L^{-1}$)	nd	nd	0.185 ± 0.020	0.156 ± 0.010	nd	nd	0.185 ± 0.020	0.174 ± 0.012
Low molecular-weight acids ($mg \cdot L^{-1}$)	nd	nd	0.020 ± 0.002	0.019 ± 0.001	nd	nd	0.020 ± 0.002	0.019 ± 0.002
Amphiphylic molecules ($mg \cdot L^{-1}$)	nd	nd	0.290 ± 0.032	0.248 ± 0.043	nd	nd	0.290 ± 0.032	0.271 ± 0.022
Polysaccharides ($mg \cdot L^{-1}$)	nd	nd	0.073 ± 0.002	0.056 ± 0.005	nd	nd	0.073 ± 0.002	0.069 ± 0.008
Phosphate ($mg \cdot L^{-1}$)	0.332 ± 0.003	0.337 ± 0.003	0.339 ± 0.003	0.323 ± 0.002	0.332 ± 0.003	0.340 ± 0.001	0.339 ± 0.003	0.329 ± 0.002
DNA concentration ($ng \cdot mL^{-1}$ of medium)	0.14	0.112 ± 0.043	nd	1.569 ± 0.348	nd	20.467 ± 2.250	nd	29.133 ± 0.879
Bacterial cell count (10^6 cells$\cdot mL^{-1}$)	1.343 ± 0.601	1.403 ± 0.627	nd	1.931 ± 0.864	nd	10.129 ± 4.530	nd	9.630 ± 4.307

Table 1 (continued).

Absorbance measurements	**B_i, D_i**	**B_f**	**D_f**	**H_i, HD_i**	**H_f**	**HD_f**
Specific UV absorbance at 254 nm [$SUVA_{254}$ (L mg-L^{-1} m^{-1})]	0.431 ± 0.085	0.188 ± 0.055	0.177 ± 0.022	3.826 ± 0.030	3.723 ± 0.050	3.775 ± 0.009
Spectral slope at 275–295 nm (nm^{-1})	0.015 ± 0.000	0.029 ± 0.014	0.032 ± 0.007	0.014 ± 0.000	0.013 ± 0.000	0.013 ± 0.000
Spectral slope at 350-400 nm (nm^{-1})	0.005 ± 0.000	0.003 ± 0.001	0.005± 0.000	0.008 ± 0.000	0.014 ± 0.001	0.013 ± 0.001
Spectral slopes ratio	0.691 ± 0.034	nd	0.811 ± 0.234	0.765 ± 0.008	0.821 ± 0.009	0.818 ± 0.009
Fluorescence measurements	**B_i, D_i**	**B_f**	**D_f**	**H_i, HD_i**	**H_f**	**HD_f**
Fluorescence index (FIX)	1.739 ± 0.218	1.524 ± 0.331	1.501 ± 0.073	1.808 ± 0.009	1.779 ± 0.020	1.798 ± 0.008
Humification index (HIX)	0.246 ± 0.018	0.226 ± 0.362	0.392 ± 0.018	0.887 ± 0.002	0.879 ± 0.003	0.877 ± 0.004
Freshness index (ß:α)	0.851 ± 0.138	1.231± 0.196	0.855 ± 0.034	0.556 ± 0.003	0.555 ± 0.003	0.550 ± 0.015
Specific fluorescence at peak A (RU L mg-C^{-1})	0.008 ± 0.001	0.010 ± 0.002	0.015 ± 0.000	0.563 ± 0.008	0.579 ± 0.007	0.574 ± 0.008
Specific fluorescence at peak B (RU L mg-C^{-1})	0.790 ± 0.011	0.330 ± 0.070	0.252 ± 0.011	0.808 ± 0.037	0.221 ± 0.009	0.343 ± 0.101
Specific fluorescence at peak C (RU L mg-C^{-1})	0.005 ±0.002	0.004 ± 0.001	0.007 ± 0.000	0.253 ± 0.004	0.264 ±0.001	0.272 ± 0.003
Specific fluorescence at peak M (RU L mg-C^{-1})	0.006 ± 0.000	0.008 ± 0.001	0.011 ± 0.000	0.303 ± 0.005	0.319 ± 0.002	0.338 ± 0.007
Specific fluorescence at peak T (RU L mg-C^{-1})	0.071± 0.002	0.076 ± 0.003	0.083 ± 0.003	0.136 ± 0.003	0.145 ± 0.003	0.155 ± 0.003

Table 2. Alpha-diversity of bacterial communities in the microcosms with additions of humic matter (**H**), *Daphnia* carcasses (**D**), humic matter and carcasses together (**HD**), and blank with no carbon sources (**B**). Values are given as means of five replicates ± standard errors, except for the initial inoculate (**I**) obtained from a single measurement, and **B** microcosms (four replicates due to low DNA content in one sample).

Microcosm	Observed OTUs	Shannon Index
I	313.4	5.00
B	234.0 ± 13.1	4.60 ± 0.27
H	217.0 ± 11.9	4.73 ± 0.20
D	189.1 ± 10.6	3.31 ± 0.24
HD	191.5 ± 6.8	3.08 ± 0.17

Table 3. Abundances (in %) of the quantitatively prominent OTUs contributing the most to the dissimilarity among the inoculum sample (**I**) and the end points of the microcosms with additions of humic matter (**H**), *Daphnia* carcasses (**D**), humic matter and carcasses together (**HD**), and blank with no carbon sources (**B**). Values are given as means of five replicates ± standard errors, except for the inoculum sample obtained from a single measurement, and **B** microcosms (four replicates due to low DNA content of two samples which were pooled).

OTU	I	B	H	D	HD	Genus	Family	Class	Phyla
1	6.84	17.80 ± 3.96	3.95 ± 0.40	45.63 ± 2.39	57.39 ± 1.41	*Pseudomonas*	*Pseudomonadaceae*	*Gammaproteobacteria*	*Proteobacteria*
2	1.31	2.90 ± 1.14	3.53 ± 0.35	15.82 ± 1.16	5.40 ± 0.38	*Duganella*	*Oxalobacteraceae*	*Betaproteobacteria*	*Proteobacteria*
3	1.33	0.76 ± 0.06	0.24 ± 0.07	9.11 ± 1.07	7.42 ± 0.32	*Flavobacterium*	*Flavobacteriaceae*	*Flavobacteriia*	*Bacteroidetes*
4	20.91	7.66 ± 0.25	9.32 ± 0.94	0.19 ± 0.02	0.57 ± 0.04	*Polynucleobacter*	*Burkholderiaceae*	*Betaproteobacteria*	*Proteobacteria*
5	0.08	0.06 ± 0.03	0.09 ± 0.03	5.83 ± 0.70	4.13 ± 0.44	*Janthinobacterium*	*Oxalobacteraceae*	*Betaproteobacteria*	*Proteobacteria*
6	0.29	0.07 ± 0.01	19.64 ± 4.40	0.27 ± 0.10	0.63 ± 0.14	*vadinHA64*	*Opitutae*	*Opitutae*	*Verrucomicrobia*
7	0.01	12.35 ± 4.10	4.61 ± 1.25	0.21 ± 0.06	0.02 ± 0.01	*Rhizobacter*	*Comamonadaceae*	*Betaproteobacteria*	*Proteobacteria*
8	0.32	7.14 ± 0.87	7.88 ± 0.80	0.03 ± 0.01	0.33 ± 0.06	*uncultured*	*uncultured*	*Thermoleophilia*	*Actinobacteria*
9	3.49	8.08 ± 1.28	4.06 ± 0.70	0.47 ± 0.03	0.30 ± 0.03	*Reyranella*	*Rhodospirillales InsSed*	*Alphaproteobacteria*	*Proteobacteria*
10	15.52	6.24 ± 0.31	0.92 ± 0.30	0.03 ± 0.01	0.03 ± 0.01	*FukuN18*	*FukuN18*	*Spartobacteria*	*Verrucomicrobia*
11	0.22	0.04 ± 0.01	0.17 ± 0.09	1.40 ± 0.15	2.81 ± 0.20	*uncultured*	*Chitinophagaceae*	*Sphingobacteriia*	*Bacteroidetes*
12	4.94	5.36 ± 0.39	2.21 ± 0.17	0.14 ± 0.01	0.20 ± 0.02	*Mycobacterium*	*Mycobacteriaceae*	*Actinobacteria*	*Actinobacteria*
13	0.14	0.07 ± 0.02	0.07 ± 0.02	1.98 ± 0.40	2.01 ± 0.67	*Pseudomonas*	*Pseudomonadaceae*	*Gammaproteobacteria*	*Proteobacteria*
15	0.00	0.60 ± 0.54	7.41 ± 4.72	0.01 ± 0.00	0.03 ± 0.01	*Aquabacterium*	*Comamonadaceae*	*Betaproteobacteria*	*Proteobacteria*
16	0.00	0.03 ± 0.02	2.63 ± 0.70	0.82 ± 0.12	0.70 ± 0.10	*Alkanibacter*	*Nevskiaceae*	*Gammaproteobacteria*	*Proteobacteria*
19	0.07	0.08 ± 0.01	0.02 ± 0.01	0.00 ± 0.00	1.86 ± 0.37	*Bacteriovorax*	*Bacteriovoracaceae*	*Deltaproteobacteria*	*Proteobacteria*
20	0.01	0.00 ± 0.00	0.05 ± 0.02	0.91 ± 0.28	0.79 ± 0.28	*OPS17*	*env.OPS_17*	*Sphingobacteriia*	*Bacteroidetes*
25	4.74	0.98 ± 0.11	0.69 ± 0.04	0.01 ± 0.00	0.03 ± 0.01	*unclassified*	*Sporichthyaceae*	*Actinobacteria*	*Actinobacteria*
28	3.60	1.43 ± 0.22	0.29 ± 0.08	0.01 ± 0.00	0.01 ± 0.00	*uncultured*	*Planctomycetaceae*	*Planctomycetacia*	*Planctomycetes*
29	2.85	1.09 ± 0.07	0.86 ± 0.07	0.01 ± 0.00	0.03 ± 0.00	*PRD01a011B*	*Methylophilaceae*	*Betaproteobacteria*	*Proteobacteria*
30	0.14	0.02 ± 0.00	2.53 ± 0.81	0.00 ± 0.00	0.09 ± 0.02	*Prosthecobacter*	*Verrucomicrobiaceae*	*Verrucomicrobiae*	*Verrucomicrobia*
33	0.00	0.00 ± 0.00	0.01 ± 0.01	0.71 ± 0.32	0.54 ± 0.33	*OPS17*	*env.OPS_17*	*Sphingobacteriia*	*Bacteroidetes*
34	0.00	0.55 ± 0.24	2.01 ± 0.82	0.00 ± 0.00	0.00 ± 0.00	*Zoogloea*	*Rhodocyclaceae*	*Betaproteobacteria*	*Proteobacteria*
39	1.96	0.16 ± 0.01	0.04 ± 0.01	0.03 ± 0.02	0.42 ± 0.06	*Flavobacterium*	*Flavobacteriaceae*	*Flavobacteriia*	*Bacteroidetes*
55	1.97	0.34 ± 0.05	0.16 ± 0.02	0.00 ± 0.00	0.01 ± 0.00	*unclassified*	*Sporichthyaceae*	*Actinobacteria*	*Actinobacteria*
64	1.42	0.12 ± 0.01	0.13 ± 0.01	0.01 ± 0.00	0.03 ± 0.01	*hgcI*	*Sporichthyaceae*	*Actinobacteria*	*Actinobacteria*

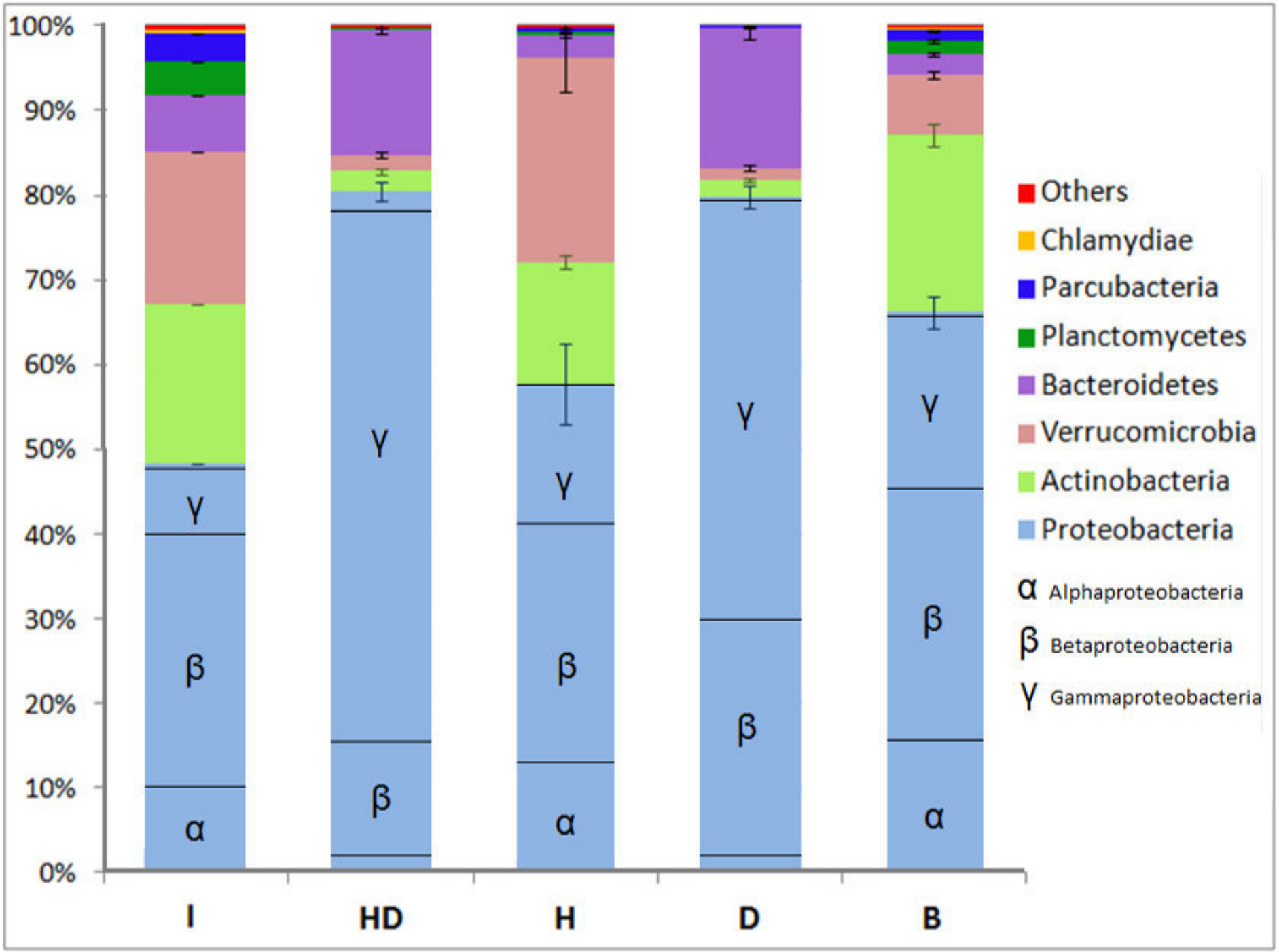
100%
90%
80%
70%
60%
50%
40%
30%
20%
10%
0%
I
HD
H
D
B
α
β
γ
Others
Chlamydiae
Parcubacteria
Planctomycetes
Bacteroidetes
Verrucomicrobia
Actinobacteria
Proteobacteria
α Alphaproteobacteria
β Betaproteobacteria
γ Gammaproteobacteria

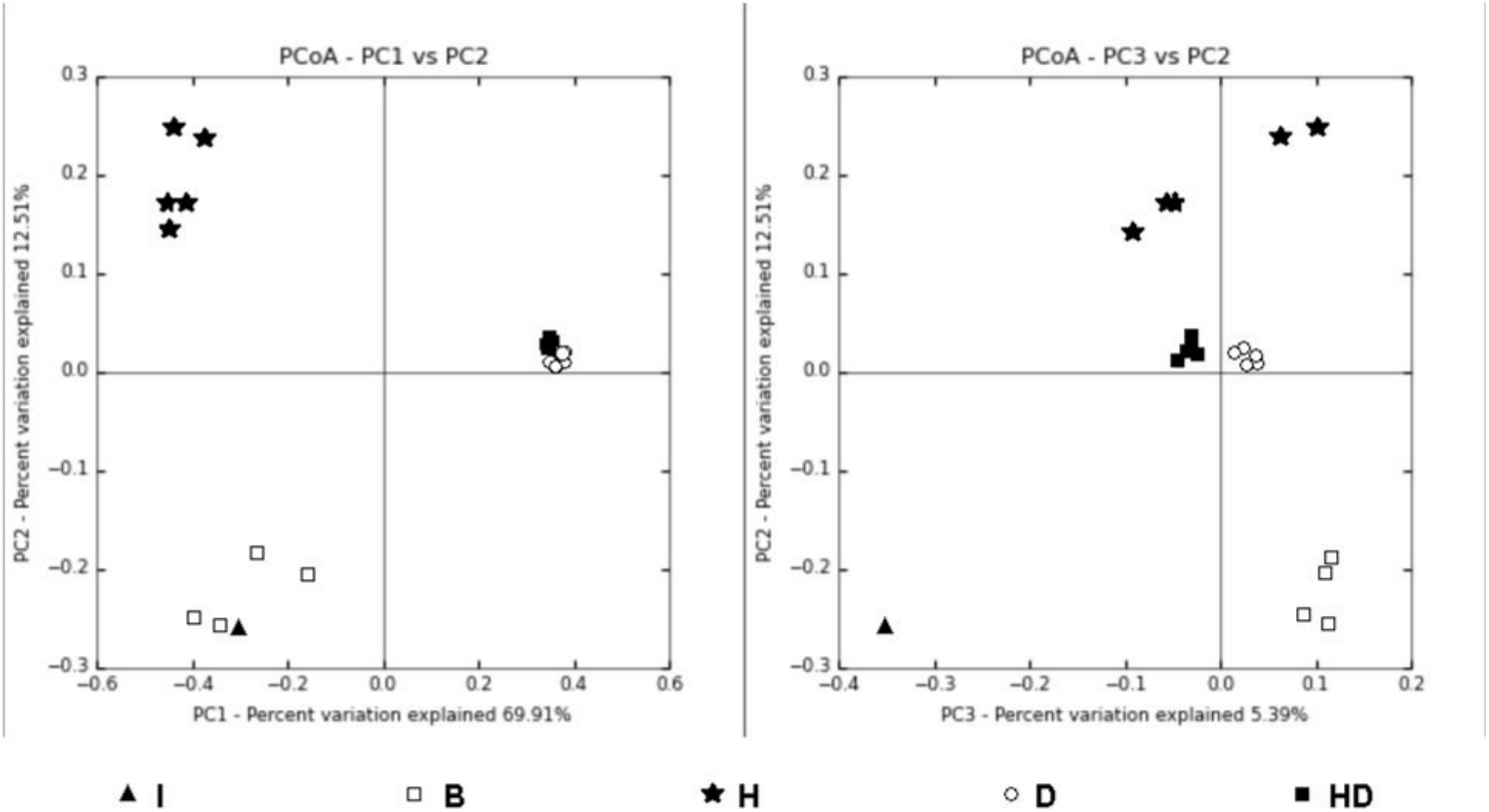
PCoA - PC1 vs PC2
PC2 - Percent variation explained 12.51%
PC1 - Percent variation explained 69.91%
PCoA - PC3 vs PC2
PC2 - Percent variation explained 12.51%
PC3 - Percent variation explained 5.39%
I
B
H
D
HD

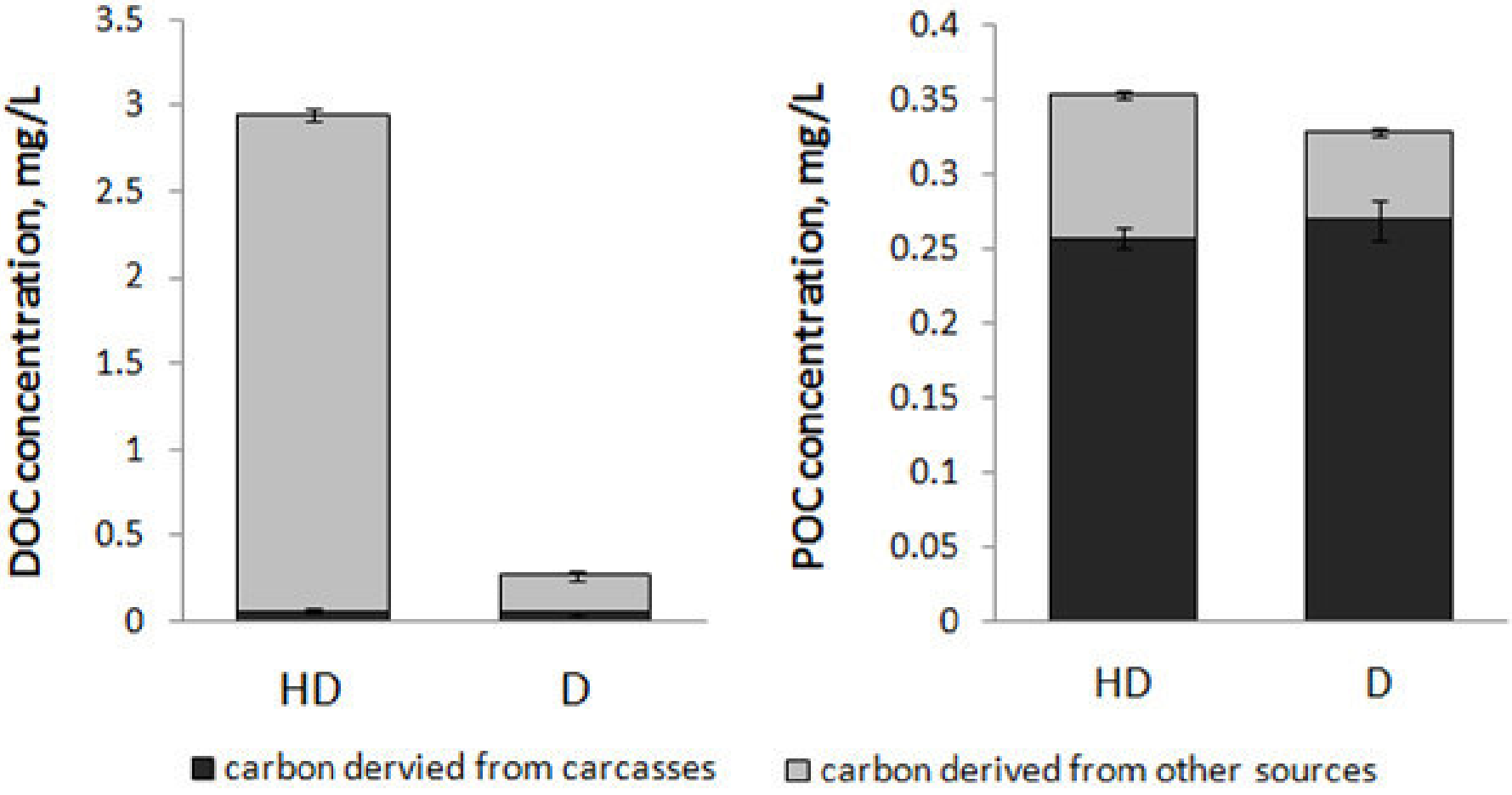
DOC concentration, mg/L
3.5
3
2.5
2
1.5
1
0.5
0
HD
D
POC concentration, mg/L
0.4
0.35
0.3
0.25
0.2
0.15
0.1
0.05
0
HD
D
carbon dervied from carcasses
carbon derived from other sources

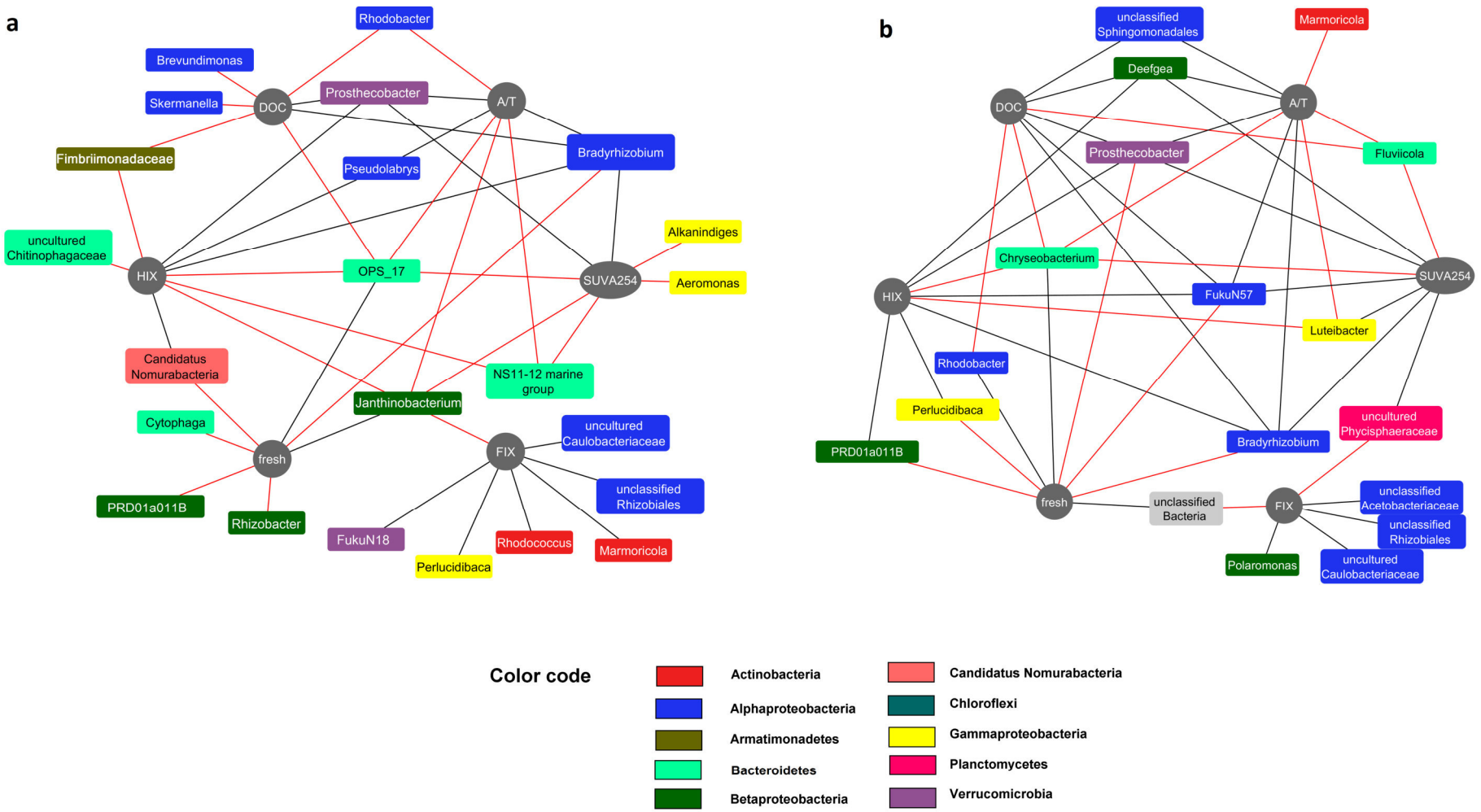
a
Rhodobacter
Brevundimonas
Skermanella
DOC
Prosthecobacter
A/T
Fimbriimonadaceae
Pseudolabrys
Bradyrhizobium
uncultured Chitinophagaceae
HIX
OPS_17
SUVA254
Alkanindiges
Aeromonas
Candidatus Nomurabacteria
NS11-12 marine group
Janthinobacterium
Cytophaga
fresh
FIX
uncultured Caulobacteriaceae
unclassified Rhizobiales
PRD01a011B
Rhizobacter
FukuN18
Perlucidibaca
Rhodococcus
Marmoricola
b
unclassified Sphingomonadales
Marmoricola
Deefgea
DOC
A/T
Prosthecobacter
Fluviicola
Chryseobacterium
SUVA254
HIX
FukuN57
Luteibacter
Rhodobacter
Perlucidibaca
uncultured Phycisphaeraceae
Bradyrhizobium
PRD01a011B
fresh
unclassified Bacteria
FIX
unclassified Acetobacteriaceae
unclassified Rhizobiales
Polaromonas
uncultured Caulobacteriaceae
Color code
Actinobacteria
Alphaproteobacteria
Armatimonadetes
Bacteroidetes
Betaproteobacteria
Candidatus Nomurabacteria
Chloroflexi
Gammaproteobacteria
Planctomycetes
Verrucomicrobia

Supplementary Information

Community composition in different microcosms

Actinobacteria and *Verrucomicrobia* had comparatively high abundances in the initial inoculum (19% and 18%, respectively), but their final abundance diverged in different treatments (Fig. 1). While in **HD** and **D** microcosms both phyla decreased down to 1-2% of total abundance, in **H** microcosms *Verrucomicrobia* increased to 24 %, and *Actinobacteria* slightly decreased to 14 % at the end of the incubation. In contrast, *Actinobacteria* increased in abundance (to 21 %) and *Verrucomicrobia* decreased (to 7 %) at the end of the incubation in the **B** microcosms (Fig. 1).

Initially, the relative abundance of *Bacteroidetes* was 7%, increasing to 15 % and 17 % in the **HD** and **D** microcosms, respectively (Fig. 1). At the end of the incubation, only 3 % of sequences in **H** microcosms and 2 % of sequences in **B** microcosms belonged to *Bacteroidetes*. Members of the candidate phylum *Parcubacteria* initially accounted for 3% of all sequences, but dropped in all treatments. All other identified phyla did not exceed a threshold of 1% in any sample.

In the bacterial inoculum from Lake Grosse Fuchskuhle, OTU4 *Polynucleobacter* sp. from the class *Betaproteobacteria* dominated (21 %, Table 3). OTU10 FukuN18 (*Verrucomicrobia*) was the second numerous OTU (16 %, Table 3) in the natural community. However, at the end of the experiment, both OTUs decreased in all microcosms, especially in the **HD** and **D** microcosms (<1%, Table 3).

In the **B** microcosms, OTU1 *Pseudomonas* from the class *Gammaproteobacteria*, which was also present in the initial sample with 7 %, became dominant (18 %), and OTU7 *Rhizobacter* (*Betaproteobacteria*) considerably increased from almost absent to 12 % (Table 3).

In the **H** microcosms, OTU4 *Polynucleobacter* decreased to 9 % of all sequences representing the second most abundant member of the community (Table 3). Instead, OTU6

27 vadinHA64 (*Opitutae, Verrucomicrobia*) became dominant (20 %) in the **H** microcosm, but
28 did not increase in any other microcosm. Microcosms **H** were characterized by higher
29 fractions of OTU15 *Aquabacterium*, OTU16 *Alkanibacter*, OTU30 *Prosthecobacter* and
30 OTU34 *Zoogloea* when compared to other microcosms.

31 In both **D** and **HD** microcosms, OTU1 *Pseudomonas* was dominant (46 % and 57 %,
32 respectively; Table 3). In the **D** microcosm, OTU2 *Duganella* (*Betaproteobacteria*) was
33 remarkably more abundant than in other treatments (16 %). OTU3 *Flavobacterium*
34 (*Bacteroidetes*) was also highly abundant in **D** and **HD** microcosms (9% and 7 %,
35 respectively). Other OTUs were enriched in the **HD** and **D** microcosms: OTU 5
36 *Janthinobacterium*, OTU11 uncultured *Chitinophagaceae*, OTU13 *Pseudomonas* (Table 3).
37 Interestingly, OTU19 *Bacteriovorax* was enriched only in the **HD** microcosms (Table 3).

38 Overall, the diversity of bacterial communities decreased with the total amount of
39 available LOM (Table 2), indicating the copiotrophic nature of the dominant
40 *Gammaproteobacteria*. Microcosms **B** (no OM addition) supported the bacterial community
41 which remained most similar to the initial inoculum **I** (Fig. 2). The dissimilarity between the
42 initial inoculum and microcosms **B** was mainly caused by the dominance of OTU4
43 *Polynucleobacter* (Table S1) in the initial sample. This group of bacteria represents a
44 common genus of freshwater bacterioplankton communities (Hahn *et al.*, 2009), and has been
45 described earlier for Lake Grosse Fuchskuhle (Hutalle-Schmelzer *et al.*, 2010). Several
46 *Polynucleobacter* clades prefer acidic lakes and have been shown to assimilate the breakdown
47 products of humic matter (Newton *et al.*, 2011), but not humic matter itself (Hutalle-
48 Schmelzer *et al.*, 2010). At the end of the experiment, *Pseudomonas* represented the most
49 dominant genus in microcosms **D** and **HD**, but was also abundant in microcosms **B** (Table 3).
50 This particular genus contributed the most to the observed differences between **HD**, **D** and all
51 other microcosms (OTU1, Table S1), but it represents a taxonomically and physiologically
52 diverse group, including putrefactive (Pekhtasheva, 2012) and chitinolytic bacteria (Gooday,

1990). Our data suggest that *Pseudomonas* are greatly favored by the presence of the relatively labile organic carbon pool derived from zooplankton carcasses indicating the high potential of carcasses to select for specific bacterial communities different from those in Lake Grosse Fuchskuhle and other lakes.

Bacterial communities of microcosms **HD** and **D** were very similar (Fig. 2) and characterized by a high abundance of copiotrophs adapted to high nutrient availability, and chitinolytic bacteria, i.e. *Flavobacterium* (Gooday, 1990; Newton *et al.*, 2011), *Janthinobacterium, Duganella* (Haack *et al.*, 2016) and uncultured representatives of *Chitinophagaceae* (Kämpfer, 2015).

In the **H** microcosms, the dominant OTU6 vadinHA64 (*Opitutae, Verrucomicrobia*, Table 3) is of a particular interest due to its ability to benefit from humic matter additions. However, only limited information is available about this so far uncultivated and uncharacterized strain.

References

Gooday, G.W. (1990). The ecology of chitin degradation. In: Marshall KC (ed). *Advances in Microbial Ecology*. Springer US: Boston, MA, pp 387–430.

Haack, F.S., Poehlein, A., Kröger, C., Voigt, C.A., Piepenbring, M., Bode, H.B., *et al.* (2016). Molecular keys to the *Janthinobacterium* and *Duganella spp.* interaction with the plant pathogen *Fusarium graminearum*. *Front Microbiol* **7**. e-pub ahead of print, doi: 10.3389/fmicb.2016.01668.

Hahn, M.W., Lang, E., Brandt, U., Wu, Q.L., Scheuerl, T. (2009). Emended description of the genus *Polynucleobacter* and the species *P. necessarius* and proposal of two subspecies, *P. necessarius subspecies necessarius subsp. nov.* and P. *necessarius subsp. a symbioticus subsp. nov. Int J Syst Evol Microbiol* **59**: 2002–2009.

77 Hutalle-Schmelzer, K.M.L., Zwirnmann, E., Krüger, A., Grossart, H-P. (2010). Enrichment
78 and cultivation of pelagic bacteria from a humic lake using phenol and humic matter
79 additions. *FEMS Microbiol Ecol* **72**: 58–73.
80 Kämpfer, P. (2015). *Sphingobacteriales ord. nov.* In: *Bergey's Manual of Systematics of*
81 *Archaea and Bacteria*. John Wiley & Sons, Ltd. e-pub ahead of print, doi:
82 10.1002/9781118960608.obm00034.
83 Newton, R.J., Jones, S.E., Eiler, A., McMahon, K.D., Bertilsson, S. (2011). A guide to the
84 natural history of freshwater lake bacteria. *Microbiol Mol Biol Rev* **75**: 14–49.
85 Pekhtasheva, E.L. (2012). Biodamage and biodegradation of polymeric materials. Smithers
86 Rapra, 258 p.

Supplementary Methods

Microcosm medium and added substrates

Artificial lake water

Artificial lake water was prepared following the protocol for acidic waters of Smith et *al.* (2002), but excluding the addition of aluminum chloride. The pH was corrected to 5.3 to match the original pH of Lake Grosse Fuchskuhle at the time of sampling. 1.6 mg L^{-1} of nitrate and 0.36 mg L^{-1} of phosphate were added to avoid nutrient limitation. Each microcosm was filled with 499 mL of artificial lake water.

Bacterial community and humic matter

The bacterial source community was obtained from the north-eastern basin of the artificially divided lake Grosse Fuchskuhle (Grossart *et al.*, 2008; Hutalle-Schmelzer *et al.*, 2010), which is fed by waters of a surrounding bog, thus most of its dissolved organic matter is composed of humic matter. After preliminary filtration of lake water through 0.8 µm for elimination of grazers as previously described in other degradation studies (Hutalle-Schmelzer *et al.*, 2010; Attermeyer *et al.*, 2014), the bacterial community was concentrated by tangential flow filtration and further centrifugation (30 min at 8000 rpm at 4°C). The bacterial pellet was then transferred to PBS buffer and kept overnight at 4 °C prior inoculation of 1 mL into each microcosm as in Attermeyer *et al.* (2014).

Humic matter previously extracted from the south-western part of Lake Grosse Fuchskuhle by reverse osmosis was used as a ROM source (Hutalle-Schmelzer *et al.*, 2010). The humic extract was diluted, filtered through 0.45 µm, and added to microcosms **HD** and **H** (mean final concentration 3.025 ± 0.070 mg C L^{-1}). The ROM added to the microcosms had a signature of $\delta^{13}C = -6.28‰$.

24 *^{13}C-labeled zooplankton carcasses*

25 A culture of *Daphnia magna* was fed with *Scenedesmus quadricauda* grown in
26 modified Z-medium (Schlösser, 1994), containing ^{13}C-labeled sodium bicarbonate (Sigma
27 Aldrich, 98 atom % ^{13}C). Just before starting the experiment, daphnids were killed by short
28 exposure to 10% acetic acid and thereafter rinsed several times in ultrapure water (Tang *et al.*,
29 2006). Carcasses were manually divided into equal groups by numbers and size, and adjusted
30 to even out the weights of individual groups before inoculation to reach a homogenous
31 distribution of both carcasses mass and length between all **HD** and **D** microcosms. We
32 selected the number of carcasses (20 per microcosm) to be as close as possible to natural
33 values (Dubovskaya *et al.*, 2003). The carbon content of a subset of acid-killed daphnids was
34 detected by a carbon analyzer Eltra SC 800 (Eltra, Germany) to estimate the surplus of carbon
35 introduced by carcasses supply.

36 **DNA extraction**

37 Zirconium and glass beads of various diameter and 0.6 mL CTAB (cetyltrimethyl-
38 ammonium bromide) buffer were added to the samples. Then 60 µl of 10% sodium dodecyl
39 sulfate (w:v), 60 µl of 10% N-Lauroylsarcosin (w:v), and 0.6 mL of pH-neutral phenol-
40 chloroform-isoamylalcohol mixture (25:24:1, v:v:v) were added. Samples were homogenized
41 on a vortexer for 10 min at highest speed and then centrifuged at 16000×g for 10 min at 4 °C.
42 The aqueous phase was transferred into new reaction tubes, washed with 1 volume of
43 chloroform-isoamylalcohol (24:1, v:v) and centrifuged at 16000×g for 10 min at 4 °C. Again,
44 the aqueous phase was transferred into new reaction tubes and mixed with 2 volumes of 30%
45 polyethylene glycol (w:v) in 1.6 M NaCl. After incubation for 1.5 h at 4 °C samples were
46 centrifuged at 17000× g for 60 min at 4 °C. The supernatant was removed and the pellet was
47 washed with 1 mL of ice-cold 70% ethanol. After centrifugation at 17000×g for 10 min the

supernatant was removed and the nucleic acid pellet was air-dried and finally dissolved in 50 µL ultra-pure water.

Sequencing data processing

Sequences with an average quality of < 25 over a 50 bp window, that were shorter than 300 bp or which contained ambiguities and homopolymer stretches of more than 8 bases were excluded from further analysis. Chimera check was performed using UCHIME (Edgar *et al.*, 2011). Taxonomy assignment of the OTUs was done using a naïve Bayesian classifier (Wang *et al.*, 2007) and the SILVA reference database v128 with a confidence threshold of 80%. All sequences classified as unknown, eukaryote, mitochondrion, chloroplast and archaea were subsequently removed. Sequences were then clustered into operational taxonomic units (OTU) using VSEARCH (Rognes *et al.*, 2016); as implemented in Mothur with a minimum sequence similarity value of 97% and global singleton sequences were removed.

Carbon decomposition calculations

The initial amount of carbon in **D** microcosms is presumed to be equal to the initial blank plus carbon of the added *Daphnia* carcasses 1.334 ± 0.038 mg L^{-1}. Accordingly, the initial amount of carbon in the **HD** microcosms, TOC_i (HD), equals to the sum of total organic carbon in **H** microcosms, TOC_i (H), and carbon of the added carcasses. Total carbon degradation throughout the experiment was calculated in each microcosm as a difference between the final and initial TOC concentration:

$$\Delta TOC = TOC_f - TOC_i \qquad \text{(Eq. 1)}$$

Predicted total degradation of carbon in HD microcosms was computed as:

$$\Delta TOC(H+D) = \Delta TOC(H) + \Delta TOC(D) - \Delta TOC(B) \qquad \text{(Eq. 2)}$$

The carcass carbon fraction (F_c) in DOC and POC was calculated from the stable isotope mixing model (Hopkins and Ferguson, 2012):

$$F_c = (d_x - d_h)/(d_c - d_h) \qquad \text{(Eq. 3)}$$

where d_x is $\delta^{13}C$ (‰) of the DOC or POC at the end of the experiment, d_c is $\delta^{13}C$ (‰) of *Daphnia* carcasses and d_h is $\delta^{13}C$ (‰) of humic matter.

Carbon respiration calculations

In parallel, we computed $^{13}CO_2$ respiration rate as a result of carcass carbon degradation in **D** microcosms, representing the difference between final concentrations of $^{13}CO_2$ in **D** and **B** microcosms:

$$^{13}\Delta CO_2(\text{carcasses}) = {}^{13}CO_2(D) - {}^{13}CO_2(B) \qquad \text{(Eq. 4)}$$

Similarly, the quantity of $^{13}CO_2$ respired from humic matter degradation in **H** microcosms was obtained from:

$$\Delta^{13}CO_2(\text{humics}) = {}^{13}CO_2(H) - {}^{13}CO_2(B) \qquad \text{(Eq. 5)}$$

Then, we predicted $^{13}CO_2$ concentration at the final point of the experiment if carcasses and humic matter were degraded together in one microcosm without any priming effect:

$$^{13}CO_2(H+D) = \Delta^{13}CO_2(\text{carcasses}) + \Delta^{13}CO_2(\text{humics}) + {}^{13}CO_2(B) = {}^{13}CO_2(D) + {}^{13}CO_2(H) - {}^{13}CO_2(B) \qquad \text{(Eq. 6)}$$

The same calculations (Eq. 3-5) were done for $^{12}CO_2$, and the predicted ratio $^{13}CO_2(H+D)/^{12}CO_2(H+D)$ was computed. The result was compared with the observed ratio $^{13}CO_2(HD)/^{12}CO_2(HD)$.

For calculating the carcass carbon fraction ($F_{c'}$) in the respired CO_2 of the **HD** microcosms we used the stable isotope mixing model:

$$F_{c'} = (d_{x'} - d_h)/(d_c - d_h) \qquad \text{(Eq. 7)}$$

where $d_{x'}$ is the $\delta^{13}C$ (‰) of the dissolved CO_2 at the end of the experiment, d_c is $\delta^{13}C$ (‰) of respired CO_2 originating from *Daphnia* carcasses, and d_h is $\delta^{13}C$ (‰) of respired CO_2 originating from humic matter.

98 **References**

99 Attermeyer, K., Hornick, T., Kayler, Z.E., Bahr, A., Zwirnmann, E., Grossart, H.-P., and
100 Premke, K. (2014) Enhanced bacterial decomposition with increasing addition of
101 autochthonous to allochthonous carbon without any effect on bacterial community
102 composition. *Biogeosciences* **11**: 1479–1489.

103 Dubovskaya, O.P., Gladyshev, M.I., Gubanov, V.G., and Makhutova, O.N. (2003) Study of
104 non-consumptive mortality of Crustacean zooplankton in a Siberian reservoir using
105 staining for live/dead sorting and sediment traps. *Hydrobiologia* **504**: 223–227.

106 Edgar, R.C., Haas, B.J., Clemente, J.C., Quince, C., and Knight, R. (2011) UCHIME
107 improves sensitivity and speed of chimera detection. *Bioinformatics.* **27**: 2194–2200.

108 Grossart, H.-P., Jezbera, J., Hornak, K., Hutalle, K.M.L., Buck, U., and Simek, K. (2008)
109 Top-down and bottom-up induced shifts in bacterial abundance, production and
110 community composition in an experimentally divided humic lake. *Environ Microbiol*
111 **10**: 635–652.

112 Hopkins, J.B. and Ferguson, J.M. (2012) Estimating the diets of animals using stable isotopes
113 and a comprehensive Bayesian mixing model. *PLoS ONE* **7**: e28478.

114 Hutalle-Schmelzer, K.M.L., Zwirnmann, E., Krüger, A., and Grossart, H.-P. (2010)
115 Enrichment and cultivation of pelagic bacteria from a humic lake using phenol and
116 humic matter additions. *FEMS Microbiol Ecol* **72**: 58–73.

117 Rognes, T., Flouri, T., Nichols, B., Quince, C., and Mahé, F. (2016) VSEARCH: a versatile
118 open source tool for metagenomics. *PeerJ* **4**: e2584.

119 Schlösser, U.G. (1994) SAG - Sammlung von Algenkulturen at the University of Göttingen
120 Catalogue of Strains 1994. *Bot Acta* **107**: 113–186.

121 Smith, E.J., Davison, W., and Hamilton-Taylor, J. (2002) Methods for preparing synthetic
122 freshwaters. *Water Res* 36: 1286–1296.

Tang, K.W., Hutalle, K.M.L., and Grossart, H. (2006) Microbial abundance, composition and enzymatic activity during decomposition of copepod carcasses. *Aquat Microb Ecol.***45**: 219–227.

Wang, Q., Garrity, G.M., Tiedje, J.M., and Cole, J.R. (2007) Naïve Bayesian classifier for rapid assignment of rRNA sequences into the new bacterial taxonomy. *Appl. Environ. Microbiol.* **73**: 5261–5267.

Supplementary Figure Legends

Fig. S1 Experimental setup with blank controls (right, **B**), single-source incubations (middle, **D** and **H**), and mixed treatments (left, **HD**). Microcosms were 1L glass bottles half-filled with artificial lake water and inoculated with a natural bacterial community. Each type of microcosm is represented by five replicates.

Fig. S2 Microscopic observations of *Daphnia magna* carcasses decomposition during the first 5 days of the experiment: **a** – Day 0; **b** – Day 1; **c** – Day 2; **d** – Day 3-5. After day 3, differences in individual carcasses conditions are noticeable. After day 5, all carcasses fell apart into pieces; **e** – DAPI-stained carcass colonized by bacterial cells at day 15.

Fig. S3 Change in concentrations of $^{12}CO_2$ and $^{13}CO_2$ compared to the blank microcosm in the final points of experimental microcosms with different organic carbon sources: humic matter (**H**), *Daphnia* carcasses (**D**), humic matter and carcasses together (**HD**).

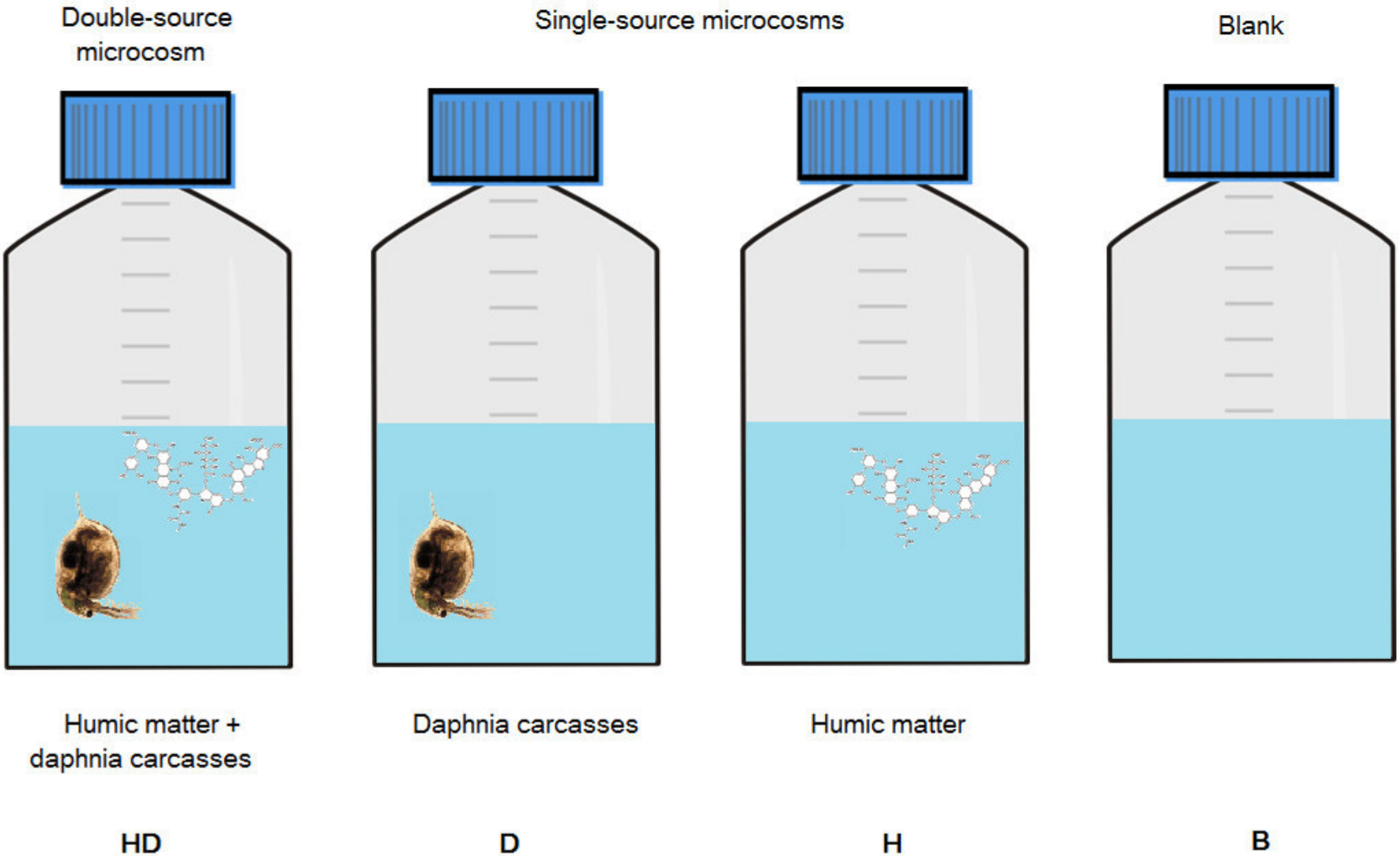
Double-source microcosm
Single-source microcosms
Blank
Humic matter + daphnia carcasses
Daphnia carcasses
Humic matter
HD
D
H
B

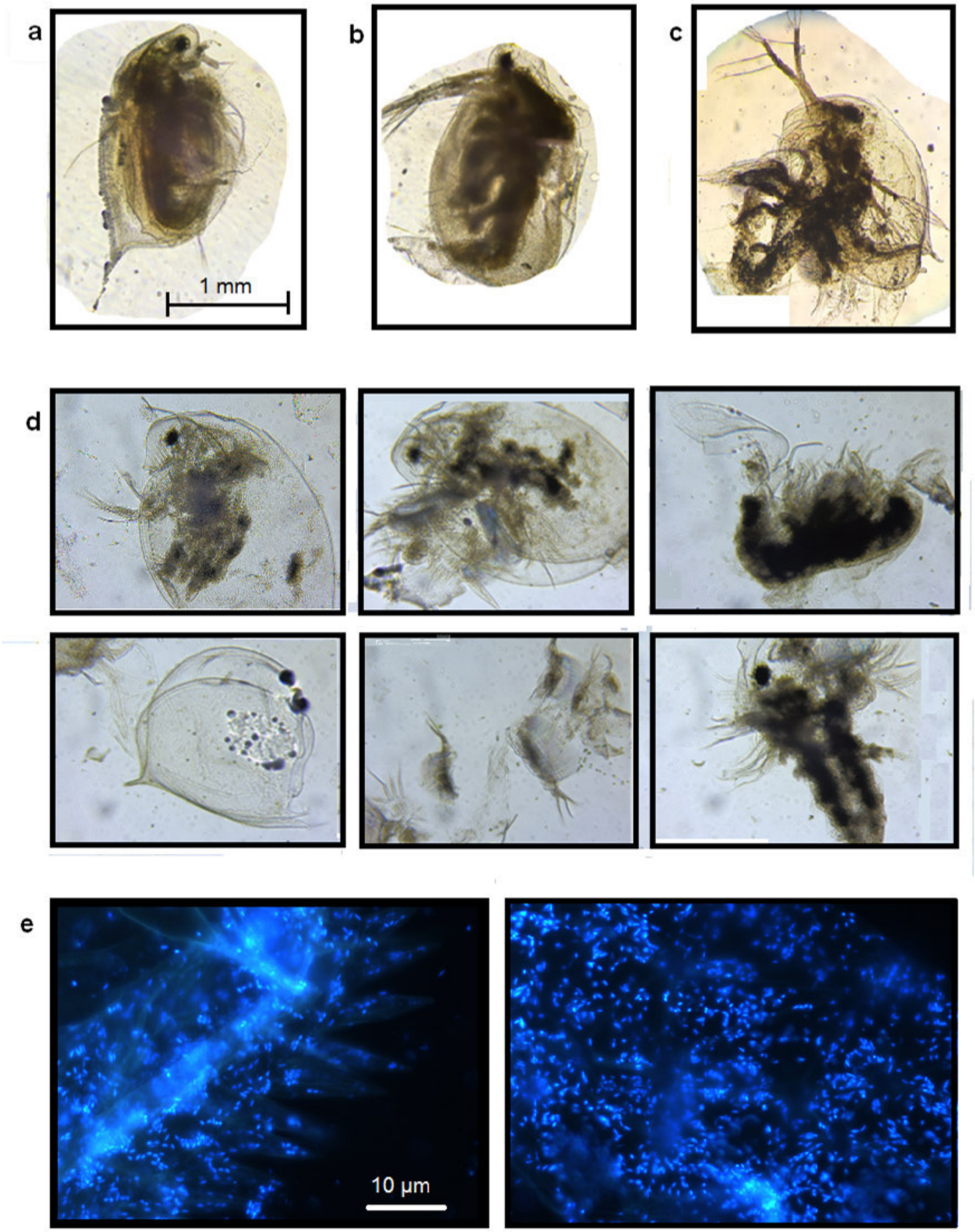
a
1 mm
b
c
d
e
10 µm

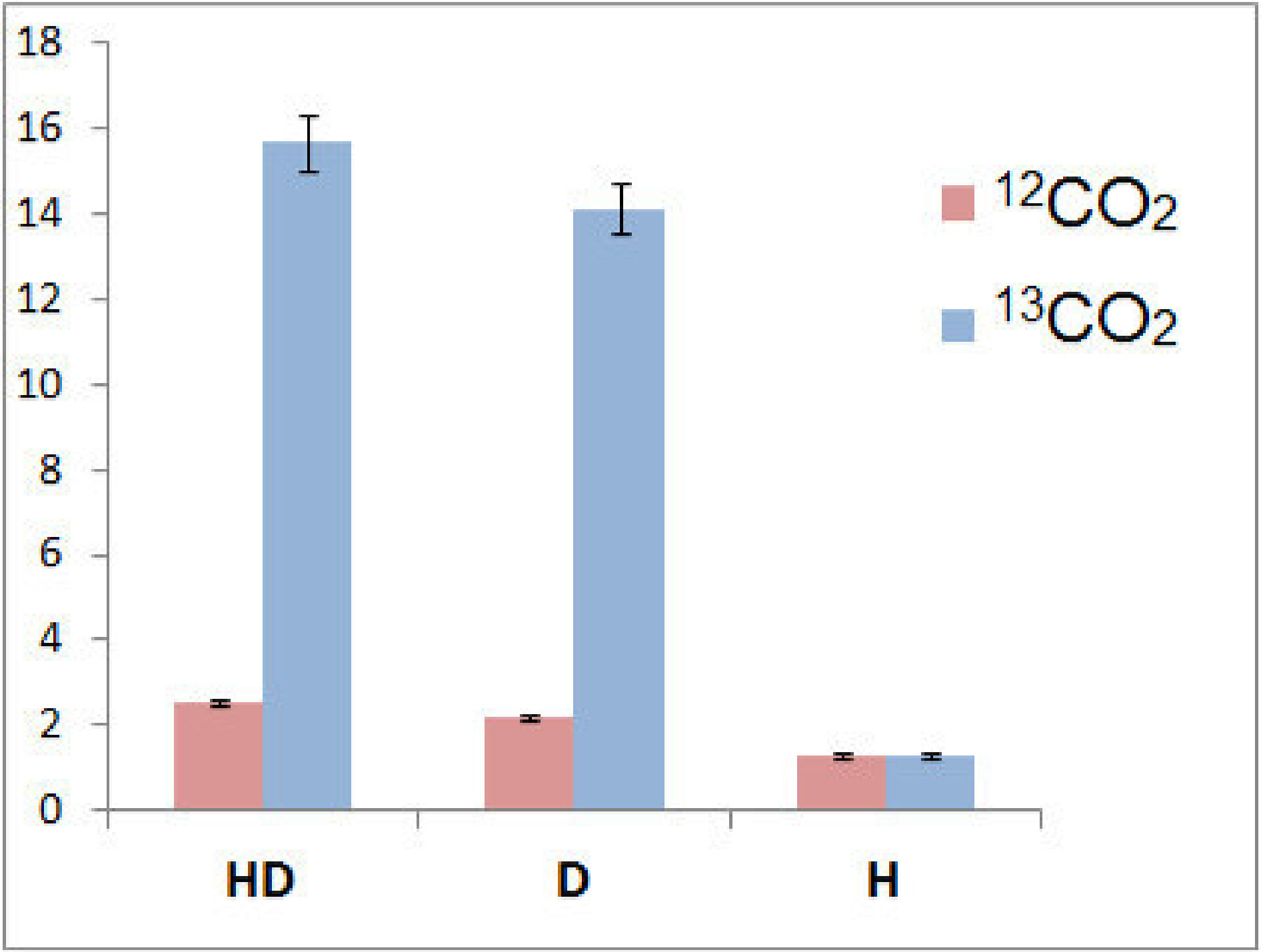
18
16
14
12
10
8
6
4
2
0
HD
D
H
$^{12}CO_2$
$^{13}CO_2$

Table S1. OTUs contributing the most to dissimilarity between the experimental microcosms according to SIMPER and significantly different at $P < 0.05$ after Tukey's test for one-way ANOVA. Treatments abbreviations: **I** – initial inoculum, **B** – blank microcosms with no carbon sources, **H -** with humic matter, **D** – with *Daphnia* carcasses, **HD** - humic matter and carcasses combined together .

	I	**B**	**H**	**D**
B	4, 10, 25, 8, 28, 29, 39, 55, 64			
H	4, 10, 6, 25, 12, 8, 28, 29, 39, 55, 64	6, 1, 10, 9, 12, 16, 30		
D	1, 4, 2, 10, 3, 5, 12, 25, 28	1, 2, 3, 7, 5, 4, 9, 8, 10	1, 2, 3, 6, 5, 4, 8	
HD	1, 4, 10, 3, 5, 25, 12, 28	1, 3, 7, 5, 9, 4, 8, 10	1, 6, 3, 5, 4, 8, 11	1, 2, 19, 11